

University of Wollongong

Research Online

Faculty of Science, Medicine and Health -
Papers: part A

Faculty of Science, Medicine and Health

1-1-2013

The Itsaq Gneiss Complex of Greenland: Episodic 3900 to 3660 Ma juvenile crust formation and recycling in the 3660 to 3600 Ma Isukasian orogeny

Allen P. Nutman
University of Wollongong, anutman@uow.edu.au

Vickie C. Bennett
Australian National University

Clark R. L Friend
Tiddington, UK

Hiroshi Hidaka
University of Hiroshima

Keewook Yi
Korea Institute of Geoscience and Mineral Resources

See next page for additional authors

Follow this and additional works at: <https://ro.uow.edu.au/smhpapers>



Part of the [Medicine and Health Sciences Commons](#), and the [Social and Behavioral Sciences Commons](#)

Recommended Citation

Nutman, Allen P.; Bennett, Vickie C.; Friend, Clark R. L.; Hidaka, Hiroshi; Yi, Keewook; Lee, Seung Ryeol; and Kamiichi, Tomoyuki, "The Itsaq Gneiss Complex of Greenland: Episodic 3900 to 3660 Ma juvenile crust formation and recycling in the 3660 to 3600 Ma Isukasian orogeny" (2013). *Faculty of Science, Medicine and Health - Papers: part A*. 1223.
<https://ro.uow.edu.au/smhpapers/1223>

Research Online is the open access institutional repository for the University of Wollongong. For further information contact the UOW Library: research-pubs@uow.edu.au

The Itsaq Gneiss Complex of Greenland: Episodic 3900 to 3660 Ma juvenile crust formation and recycling in the 3660 to 3600 Ma Isukasian orogeny

Abstract

From the 3000 km² Eoarchean Itsaq Gneiss Complex (IGC) of Greenland, zircon U-Pb dating of numerous meta-granitoid and orthogneiss samples is integrated with geologic observations, whole rock geochemistry and a strategic subset of zircon Hf and whole rock Nd isotopic measurements. This shows that there are multiple episodes of TTG suite formation from ~3890 to 3660 Ma, characterized by zircon initial $\epsilon_{\text{Hf}} \approx 0$ and whole rock initial ϵ_{Nd} of $> +2$. These rocks mostly have geochemical signatures of partial melting of eclogitized mafic sources, with a subset of high magnesian, low silica rocks indicating fusion by fluid fluxing of upper mantle sources. The TTG suites are accompanied by slightly older gabbros, basalts and andesites, which have geochemical signatures pointing to magmas originating from fluid fluxing of upper mantle sources. The data show the formation of juvenile crust domains in several discrete events from ~3900 to 3660 Ma, probably at convergent plate boundaries in an environment analogous, but not identical to, modern island arcs.

In the Isua area, a northern ~3700 Ma terrane formed distal from a predominantly ~3800 Ma terrane. These terranes were juxtaposed between 3680 and 3660 Ma—respectively the age of the youngest rocks unique to the northern terrane and the lithologically distinctive ultramafic-granitic Inaluk dykes common to both terranes. This shows the assembly of different domains of juvenile rocks to form a more expansive domain of “continental” crust. A rare occurrence of high-pressure granulite is dated at ~3660 Ma, demonstrating that assembly involved tectonic crustal thickening.

This continental crust was then reworked in the 3660 to 3600 Ma Isukasian orogeny. In the northern part of the Isua area, 3660 to 3600 Ma granites were emplaced into ~3700 Ma tonalites. The earliest granites are nebulous, and sigmoidal schlieric inclusions within them demonstrate ductile extension. Younger granite sheets were emplaced into extensional ductile-brittle fractures. These granite-tonalite relationships are overprinted by widespread development of late Eoarchean (pre-3500 Ma Ameralik dyke) brittle-ductile extensional cataclastic textures, together demonstrating that extension was polybaric. The southern part of the Isua area largely escaped 3660 to 3600 Ma high temperature processes and has sparse granite sheets commonly focused into coeval shear zones. In the rest of the complex, deeper crustal levels during the Isukasian orogeny are widely preserved. These experienced upper amphibolite to granulite facies moderate- to low-pressure syn-kinematic metamorphism, forming complex migmatites rich in granitic-trondhjemitic neosome. The migmatites were intruded by composite ferrogabbro and granite bodies, in which syn-magmatic extensional features are locally preserved. Thus 3660 to 3600 Ma crustal recycling involved elevated crustal thermal gradients in an extensional regime. Crustal melts formed in the Isukasian orogeny have zircon initial ϵ_{Hf}

Keywords

juvenile, crust, formation, episodic, 3600, 3920, recycling, itsaq, gneiss, complex, southern, west, greenland, 3660, ma, GeoQuest

Disciplines

Medicine and Health Sciences | Social and Behavioral Sciences

Publication Details

Nutman, A. P., Bennett, V. C., Friend, C. R. L., Hidaka, H., Yi, K., Lee, S. & Kamiichi, T. (2013). The Itsaq Gneiss Complex of Greenland: Episodic 3900 to 3660 Ma juvenile crust formation and recycling in the 3660 to 3600 Ma Isukasian orogeny. *American Journal of Science: an international earth science journal*,

313 (9), 877-911.

Authors

Allen P. Nutman, Vickie C. Bennett, Clark R. L. Friend, Hiroshi Hidaka, Keewook Yi, Seung Ryeol Lee, and Tomoyuki Kamiichi

1 **AMERICAN JOURNAL OF SCIENCE DOI: 10.2475/09.2013.00**

2 **THE ITSAQ GNEISS COMPLEX OF GREENLAND: EPISODIC**
3 **3900-3660 Ma JUVENILE CRUST FORMATION AND**
4 **RECYCLING IN THE 3660-3600 Ma ISUKASIAN OROGENY**

5
6 ALLEN P. NUTMAN*†, VICKIE C. BENNETT**, CLARK R.L. FRIEND***,
7 HIROSHI HIDAKA[§], KEEWOOK YI^{§§}, SEUNG RYEOL LEE^{§§§}, TOMOYUKI KAMIICHI[§]

8

9 * GeoQuEST Research Centre, School of Earth & Environmental Sciences, University of
10 Wollongong, Wollongong, NSW 2522, Australia

11 ** Research School of Earth Sciences, Australian National University, Canberra, ACT 0200,
12 Australia

13 *** Glendale, Albury View, Tiddington, Oxon, OX9 2LQ, UK

14 [§] Department of Earth and Planetary Systems Sciences, University of Hiroshima,
15 1-3-1 Kagamiyama, Higashi-Hiroshima 739-8526, Japan

16 ^{§§} Geological Research Division, Korea Institute of Geoscience and Mineral Resources,
17 Daejeon 305-350, Korea

18 ^{§§§} Korean Institute of Geoscience and Mineral Resources, Daejeon 305-350, Korea

19

20 † Corresponding author: Allen Nutman (*e-mail:anutman@uow.edu.au*)

21

22

23 **ABSTRACT. From the 3000 km² Eoarchean Itsaq Gneiss Complex (IGC) of Greenland,**
24 **zircon U-Pb dating of numerous meta-granitoid and orthogneiss samples is integrated**
25 **with geologic observations, whole rock geochemistry and a strategic subset of zircon Hf**
26 **and whole rock Nd isotopic measurements. This shows that there are multiple episodes of**
27 **TTG suites formed from ~3890 to 3660 Ma, characterised by zircon initial $\epsilon_{\text{Hf}} \approx 0$ and**
28 **whole rock initial ϵ_{Nd} of $>+2$. These rocks mostly have geochemical signatures of partial**
29 **melting of eclogitised mafic sources, with a subset of high magnesian, low silica rocks**
30 **indicating fusion by fluid fluxing of upper mantle sources. The TTG suites are**
31 **accompanied by marginally older gabbros, basalts and andesites, which have**
32 **geochemical signatures pointing to magmas originating from fluid fluxing of upper**
33 **mantle sources. The data show the formation of juvenile crust domains in several discrete**
34 **events from ~3900 to 3660 Ma, probably at convergent plate boundaries in an**
35 **environment analogous, but not identical to, modern island arcs.**
36 **In the Isua area, a northern ~3700 Ma terrane formed distal from a predominantly ~3800**
37 **Ma terrane. These terranes had been juxtaposed between 3680 and 3660 Ma –**
38 **respectively the age of the youngest rocks unique to the northern terrane and the**
39 **lithologically distinctive ultramafic-granitic Inaluk dykes common to both terranes. This**
40 **shows the assembly of different domains of juvenile rocks to form a more expansive**
41 **domain of ‘continental’ crust. A rare occurrence of high-pressure granulite is dated at**
42 **~3660 Ma, demonstrating that assembly involved tectonic crustal thickening.**
43 **This continental crust was then reworked in the 3660-3600 Ma *Isukasian orogeny*. In the**
44 **northern part of the Isua area, 3660-3600 Ma granites were emplaced into ~3700 Ma**
45 **tonalites. The earliest granites are nebulous, and sigmoidal schlieric inclusions within**
46 **them demonstrate ductile extension. Younger granite sheets were emplaced into**
47 **extensional ductile-brittle fractures. These granite-tonalite relationships are overprinted**
48 **by widespread development of late Eoarchean (pre-3500 Ma Ameralik dyke)**
49 **brittle-ductile extensional cataclastic textures, together demonstrating that extension was**
50 **polybaric. The southern part of the Isua area largely escaped 3660-3600 Ma high**
51 **temperature processes and has sparse granite sheets commonly focused into coeval shear**
52 **zones. In the rest of the complex, deeper crustal levels during the Isukasian orogeny are**
53 **widely preserved. These experienced upper amphibolite to granulite facies moderate- to**
54 **low-pressure syn-kinematic metamorphism, forming complex migmatites rich in**
55 **granitic-trondhjemitic neosome. The migmatites were intruded by composite**

56 **ferrogabbro and granite bodies, in which syn-magmatic extensional features are locally**
57 **preserved. Thus 3660-3600 Ma crustal recycling involved elevated crustal thermal**
58 **gradients in an extensional regime. Crustal melts formed in the Isukasian orogeny have**
59 **zircon initial $\epsilon_{\text{Hf}} < 0$ and whole rock initial ϵ_{Nd} of ≤ 0 , showing incorporation of slightly**
60 **older Eoarchean juvenile crust. A Phanerozoic example of collisional orogeny followed**
61 **by crustal thinning is explored as an analog for the Isukasian orogeny.**

62 **Keywords:** Itsaq gneiss complex (Greenland), Eoarchean, Juvenile crust, Crustal recycling,
63 Convergent plate boundaries, Crustal extension, Isukasian orogeny
64

65

66

INTRODUCTION

67

68

69

70

71

72

73

74

75

76

77

78

79

80

81

82

Known Eoarchean (4000-3600 Ma) rocks comprise only about 1 millionth of Earth's surface, which reflects the small volume that has survived more than 3.5 billion years of plate tectonics, weathering and erosion (Nutman, 2006 and references therein). These rocks occur in several gneiss complexes scattered around the globe, and they all show broadly similar lithologies and evolutionary histories (see Schiøtte and others, 1989a; Nutman and others, 1991, 1996; Kinny and Nutman, 1996; Bowring and Williams, 1999; Iizuka and others, 2007; Liu and others, 2007; O'Neil and others, 2007 and Horie and others 2010, for accounts of the most studied occurrences). However the Itsaq Gneiss Complex (IGC) of the Nuuk district of southern West Greenland (Fig. 1; Nutman and others, 1996 and references therein) is the best exposed, and contains some rare areas of low total strain and relatively low (epidote-amphibolite facies) metamorphic overprint. The combination of these factors means that, since the antiquity of the Greenland rocks was first demonstrated by McGregor (1968, 1973), Black and others (1971), Moorbath and others (1972) and Baadsgaard (1973)¹, they have remained at the forefront in understanding the Eoarchean Earth.

83

84

85

86

87

88

89

90

91

92

93

This paper takes a holistic view of knowledge on the Eoarchean Earth accrued from the IGC and focuses on the formation environment of juvenile crust from ~3900 to 3660 Ma and the nature and setting of its recycling in the *Isukasian orogeny* between 3660-3600 Ma. Although we synthesise much published data from different sources, we also complete a U-Pb zircon SHRIMP geochronological survey of meta-granitoids and orthogneisses throughout the IGC (over 160 samples) and provide new geological information and zircon dating that gives greater insight on the 3660-3600 Ma Isukasian orogeny. Appraisal of the IGC points to >200 million years of juvenile crust formation occurring in arc-like intra-oceanic settings (≥ 3900 Ma to ~3660 Ma), then an orogeny starting with collision and crustal thickening, followed by crustal thinning with an elevated geothermal gradient. Figure 2 is a schematic flow diagram illustrating the

¹ These rocks were originally known as the *Amîtsoq gneisses* (McGregor, 1973), with the plurality deliberately chosen to indicate their already recognized lithological diversity. This term was modified into the singular *Amîtsoq gneiss* in some later publications (e.g., Kamber and Moorbath, 1998) – perhaps compatible with the interpretations therein of these rocks as a product of a single crust-forming event, rather than having formed via a more protracted series of unrelated events. In order to counter any

94 early period of juvenile crust production, followed by orogeny starting with tectonic
95 crustal thickening and then by crustal recycling coeval with extension. Figures 3A-C
96 present schematic cross sections through the upper, middle and lower parts of the crust
97 at the end of the orogeny, whereas Figure 3D shows how these sections might be
98 related. This pattern of crust formation and reworking has similarities to that seen in
99 Phanerozoic terranes, and implicates plate tectonic processes in the formation of
100 Eoarchean crust. A possible Phanerozoic analog for the Isukasian orogeny is explored.

101

102

THE ITSAQ GNEISS COMPLEX

103

Overview

104

105 Much of the IGC was affected by 3660-3600 Ma high-grade metamorphism
106 and ductile deformation (Griffin and others, 1980, Nutman and others, 1996; Friend
107 and Nutman 2005a) such that by 3600 Ma the existing lithologies had been widely
108 converted into strongly deformed multi-component amphibolite-granulite facies
109 gneisses (Fig. 4A). An additional complication in interpreting the IGC is that it occurs
110 as tectonic slivers bounded by folded Meso- and Neoproterozoic meta-mylonites, within a
111 collage of younger Archean terranes that were assembled into their present
112 configuration by the end of the Archean (Friend and others, 1987, 1988; Nutman and
113 others, 1989, Nutman and Friend, 2007; Crowley, 2002; Friend and Nutman, 2005b).
114 Thus the Eoarchean rocks are allochthons of largely strongly deformed rocks found
115 within a Neoproterozoic orogen (McGregor and others, 1991; Friend and Nutman 2005b).
116 The present extent of the IGC is ~3000 km², and runs obliquely across the coastal
117 fringe, so that in the north it disappears under the Inland Ice in the Isua supracrustal
118 belt area and the most southern exposures are on the Davis Strait coast in the Tre
119 Brødre area (Fig. 1).

119

120 The later Archean tectonothermal overprints mean that at most localities it is
121 hard to extract any detailed information concerning the early history of the IGC.
122 Fortunately, particularly around the *Isua supracrustal belt* at the IGC's northern
123 extremity (Figs. 1 and 5), there are some domains of lower strain and lower
124 metamorphic grade. This means that individual Eoarchean crustal components can be
125 sampled separately (Fig. 4B) and disturbance of whole rock geochemistry and isotopic
126 systems by superimposed events is diminished. Samples from these domains provide

perception of uniformity in these rocks, the late Vic McGregor and his colleagues introduced the term
Itsaq Gneiss Complex (Nutman, and others, 1996; with *Itsaq* being Greenlandic for *ancient thing*).

126 the most robust information on the Eoarchean Earth (e.g., Baadsgaard and others,
127 1986a; Nutman and others, 1996, 1999; Friend and others, 2002; Crowley and others,
128 2002; Crowley, 2003; Polat and Hofmann, 2003; Bennett and others, 1993, 2003,
129 2007; Hiess and others, 2009; Hoffmann and others, 2010; Nagel et al. 2012).

130 More than 95% of the IGC consists of quartzo-feldspathic rocks, now mostly
131 occurring as strongly deformed orthogneisses. The rare areas of relatively little
132 deformation show that these gneisses usually formed from plutonic tonalite and
133 younger granite (*sensu stricto*) components (Fig. 4B), with lesser amounts of volcanic
134 rocks (Nutman and others, 1996, 1997a, 2011; Bohlar and others, 2004, 2005). All
135 researchers (e.g., Steenfelt and others, 2005) indicate that the tonalites are
136 compositionally similar to the Archean tonalite-trondhjemite-granodiorite (TTG)
137 suites worldwide. The age of the tonalites ranges from at least 3850 Ma (occurring at
138 several localities) to 3660 Ma in the vicinity of Amiiitsoq (Fig. 1). The true granites
139 formed largely by partial melting of crust dominated by tonalite (Baadsgaard and
140 others, 1986a; Nutman and Bridgwater, 1986; Hiess and others, 2011).

141 Volcanic and sedimentary (supracrustal) rocks form <5% of the IGC and are in
142 tectonic slivers and as enclaves scattered within the more voluminous plutonic rocks.
143 These rocks range in size from the 35-km long Isua supracrustal belt (see Allaart 1976;
144 Nutman and Friend 2009), down to sub-metre-sized pods (e.g., McGregor and Mason
145 1977; Nutman and others, 2002a). They are dominated by banded and meta-volcanic
146 amphibolites that are commonly skarn-bearing, with lesser amounts of
147 quartz-magnetite banded iron formation (BIF), siliceous rocks and marbles.
148 Preservation of original structures and textures is rare. The BIF, siliceous rocks and
149 marbles have together been interpreted as a variegated suite of chemical sediments
150 (Allaart 1976; Nutman and others 1984a, 2010; Dymek and Klein, 1988; Dauphas and
151 others, 2004; Bohlar and others, 2004; Friend and others, 2007; Craddock and
152 Dauphas, 2011). An alternative school of thought regards the carbonates as entirely
153 metasomatic in origin, without sedimentary protoliths (Rosing and others, 1996).
154 Felsic schists and pelites of volcano-sedimentary origin also occur in the Isua
155 supracrustal belt (e.g., Nutman et al. 1984a, 1997a, 2011; Bohlar and others, 2005;
156 Kamber and others, 2005). Bodies of metagabbro locally grading into anorthosites are
157 fragments of layered (basic) intrusions, and are spatially associated with layered
158 meta-peridotites (Chadwick and Crewe 1986; Nutman and others, 1996; Friend and
159 others, 2002). Other ultramafic rocks are more magnesian, with very low alumina and

160 lime. They are found largely as metasomatized amphibole \pm phlogopite-bearing
161 schists, within which are rare small pods of non-metasomatized fine-grained dunite
162 and harzburgite. These are interpreted as upper mantle rocks tectonically intercalated
163 with supracrustal rocks, prior to the intrusion of juvenile tonalite suites (Nutman and
164 others, 1996; Friend and others, 2002; Friend and Nutman 2011).

165 In and around the Isua supracrustal belt are most of the world's occurrences of
166 Eoarchean rocks preserved in a low strain state. Additionally, the Isua area as a whole
167 has experienced lower grade metamorphism compared with other parts of the IGC
168 (Griffin and others, 1980; Nutman and others, 1996). North of line "N" in Figure 5 (see
169 the figure caption for explanation of this line), ~3500 Ma Ameralik dykes are weakly
170 to non-deformed, showing that Neoproterozoic deformation is generally low (Bridgwater
171 and McGregor 1974; Allaart, 1976). These low strain domains also reveal that *in situ*
172 melting was uncommon at the northern end of the IGC, which greatly aids the
173 interpretation of the early history of these rocks (Nutman and others, 1996).

174 Much of the rest of the IGC south of line 'N' in Figure 5 was strongly deformed
175 and highly metamorphosed at both 3660-3600 Ma in the Isukasian orogeny and during
176 later Archean tectonothermal events (Nutman, 1984). Nevertheless, there are some
177 domains that escaped both the stronger 3660-3600 Ma and later deformation. These
178 domains provide additional valuable insight into the evolution of the IGC. Thus south
179 of Nuuk in the intersections between the axial regions of Neoproterozoic recumbent and
180 superimposed upright folds, the 3660-3600 Ma characteristics of migmatites are well
181 preserved (Fig. 4A). Additionally, within a suite of ~3640 Ma coeval granites and
182 gabbros in the coastal region south of Ameralik (Fig. 1) there are domains of low later
183 Archean deformation with preserved syn-magmatic textures and structures.

184

185

186

The Isua supracrustal belt

187

188

189

190

191

192

193

194

195

196

197

198

199

200

201

202

203

204

205

206

207

208

209

210

211

212

213

214

215

216

217

218

Despite the fact the Isua supracrustal belt (Fig. 5) largely escaped strong deformation in the Neoproterozoic, most of it was strongly deformed in the Eoarchean (Nutman and others, 1984a, 1996, 2002b; Myers, 2001). Thus, in most places, primary volcanic and sedimentary structures were obliterated, and outcrop-scale compositional layering is dominantly of transposed tectonic origin. The rare low strain zones indicate that protoliths for most Isua rocks were water-lain, including pillow lavas and breccias (Komiya and others, 1999; Solvang, 1999; Furnes and others, 2007) as well as the chemical sedimentary rocks and also graded felsic detrital rocks derived from volcanic sources (Nutman and others, 1984a, 2011). Plutonic rocks are much less common, but include some gabbros and ultramafic rocks derived from both layered gabbro intrusions and the mantle (e.g. Dymek and others, 1988; Friend and Nutman, 2011).

The earliest age constraints for the Isua supracrustal belt rocks were provided by Rb-Sr whole rock Eoarchean errorchrons (linear scatters of data which give an approximate ages with errors of >50 million years) for orthogneiss components invading and proximal to the belt (e.g. Moorbath and others, 1972, 1977); a whole rock Pb-Pb 3710 ± 70 Ma errorchron on a BIF (Moorbath and others, 1973); and a Sm-Nd 3770 ± 42 Ma errorchron for a mixed suite of felsic and mafic rocks (Hamilton and others, 1978). Within the poor resolution of this early geochronological framework, it was considered that the Isua supracrustal rocks were all related. A subsequent SHRIMP U-Pb zircon-dating programme with $\leq \pm 5$ Ma uncertainties for rock ages demonstrated that the belt contained supracrustal rocks varying in age by ~100 million years, with the southern part of the belt dominated by ~3800 Ma rocks, whereas its northern and central portions contains ~3700 Ma rocks (Figs. 2 and 5; Nutman and others, 1996, 1997a, Crowley 2003; Kamber and others, 2005). Nutman and others (1997a) first proposed that these unrelated sequences were separated by Eoarchean mylonites and they have expanded on this in more recent work (Nutman and Friend, 2009; Nutman and others, 2009). Despite some adherence to the idea that the belt comprises rocks of the same age (e.g. Moorbath, 1994, 2005), most recent workers have now adopted this interpretation (e.g., Pope and others, 2012; Rizo and others, 2012).

Detailed evolution of the ~3700 Ma portion of the Isua supracrustal belt

219 As the youngest extensive and overall least deformed supracrustal assemblage
220 in the IGC, the ~3700 Ma assemblage along the northern side of the Isua supracrustal
221 belt is the most amenable to provide information on the evolution of Eoarchean
222 volcano-sedimentary sequences (Nutman and others, in press). The 3700 Ma
223 assemblage comprises tectonically imbricated slices of mostly strongly deformed,
224 amphibolitized pillow lavas and lesser amounts of gabbro (island arc tholeiite, picrite
225 and boninite protoliths; e.g., Polat and others, 2002; Polat and Hofmann, 2003), felsic
226 schists (andesite-dacite protoliths; e.g., Nutman and others, 1984a, 1997a, 2011;
227 Rosing, 1999; Bohlar and others, 2005), chemical sedimentary rocks (Allaart 1976;
228 Friend and others, 2007), and depleted mantle dunite (Friend and Nutman, 2011). In a
229 rare low strain area in the northwestern end of the belt (65°08.649'N 50°10.488'W;
230 datum WGS-84), layered gabbro, with amphibolitized relict igneous texture, occurs
231 with boninitic pillow lavas and contains high Th/U igneous zircons with an age of
232 3717 ± 19 Ma (Nutman and Friend, 2009). Boninitic amphibolites with relict pillow
233 structure are cut by a 3712 ± 6 Ma hypabyssal tonalite sheet, and an
234 amphibolite-ultramafic schist tectonic contact is transgressed by a 3717 ± 6 Ma mafic
235 tonalite intrusion (Friend and Nutman, 2010). Strongly deformed felsic schists of
236 likely volcanic origin contain 3720-3700 Ma igneous zircons, showing they are
237 marginally younger than the intercalated mafic volcanic rocks (Nutman and others,
238 2009). 3720-3710 Ma rocks are intruded by voluminous, less mafic, 3696 ± 6 Ma
239 tonalite. All samples from the ~3700 Ma assemblage have juvenile crustal isotopic
240 signatures, with whole rock initial ϵ_{Nd} values of $\geq +1$ (Baadsgaard and others, 1986a;
241 Jacobsen and Dymek, 1987; data in Moorbath, 2005; Bennett and others, 2007;
242 Hoffmann and others, 2010), and zircon initial ϵ_{Hf} values of ~ 0 (Hiess and others,
243 2009; Kemp and others, 2009; Amelin and others, 2011).

244

245 *Orthogneiss complexes adjacent to the Isua supracrustal belt*

246 The Isua supracrustal belt is bounded to the north by orthogneisses, whose
247 main components are ~3710 Ma (less abundant) and 3700-3690 Ma (more common)
248 tonalites, and several suites of 3660-3630 Ma granites and pegmatites (Nutman and
249 Bridgwater 1986; Nutman and others, 1996, 2000, 2002b; Crowley and others, 2002).
250 An Eoarchean shear zone (Nutman, 1984; Crowley and others, 2002; Nutman and
251 Friend, 2009; Nutman and others, 1997a, 2002b) separates most of these tonalites from

252 the Isua supracrustal belt (Fig. 5). Between 3660-3600 Ma the tonalites were invaded
253 by multiple generations of granites and pegmatites (Figs. 3B, 4B). These show varying
254 textural and structural relationships with the host tonalites, and new observations on
255 this are presented below, which provide insight into tectonothermal conditions during
256 the 3660-3600 Ma Isukasian orogeny.

257 Although superficially similar in the field, meta-tonalites and their gneissic
258 equivalents on the south side of the Isua supracrustal belt are older than those to the
259 north, with ages of 3820-3795 Ma (Nutman and others, 1996, 1999, 2000; Crowley
260 2003; Amelin and others, 2011). In the southern ~3800 Ma tonalite area there are
261 3660-3630 Ma granitic sheets, but they are less voluminous than granite sheets cutting
262 the tonalites to the north, and tend to be focussed into discrete syn-granite shear zones
263 (Fig. 3B).

264

265 *Tectonic intercalation related to Eoarchean crustal evolution*

266 In the Isua supracrustal belt, rocks of different age and origin are tectonically
267 juxtaposed along mylonites that were then folded (Nutman and others, 2002b; Nutman
268 and Friend, 2009). Mylonites within the eastern part of the Isua supracrustal belt and
269 along its northern margin are Eoarchean in age, because Ameralik dykes that extend
270 across tectonic contacts have U-Pb zircon and baddeleyite ages of ~3500 Ma (White et
271 al., 2000; Nutman et al., 2004a, 2007a; Nutman and Friend, 2009). Further detailed
272 tectonic studies integrated with U-Pb zircon dating of the northern ~3700 Ma portion
273 of the belt have revealed a sequence of intercalation events, starting from ≥ 3710 Ma
274 prior to the completion of juvenile crust formation, through 3690-3660 Ma collision
275 with the southern ~3800 Ma terrane, to 3660-3600 Ma post-assembly shearing
276 (Crowley and others, 2002; Nutman and Friend, 2009; Friend and Nutman, 2011).

277

278

279 MILESTONES IN UNDERSTANDING THE CRUSTAL DYNAMICS OF THE
280 EOARCHEAN EARTH FROM THE ITSAQ GNEISS COMPLEX

281 A series of now broadly-accepted findings from the IGC provide robust
282 information on Eoarchean crust formation, lithospheric dynamics and orogeny and
283 include:

284

285 *Eoarchean crust formed in the Archean, and is not recycled Hadean continental crust*

286 The first Rb-Sr isotopic studies of IGC orthogneisses of what then were the
287 only-known Eoarchean rocks (Moorbath and others, 1972; Moorbath 1975)
288 recognized that their primitive isotopic signatures (i.e. low initial $^{87}\text{Sr}/^{86}\text{Sr}$) meant they
289 represented predominantly igneous rocks derived from material separated from the
290 mantle only shortly beforehand. Hence they are *not* material recycled from appreciably
291 older Hadean (>4000 Ma) rocks. Numerous isotopic studies using first whole rock
292 Rb-Sr and Pb-Pb, then whole rock Sm-Nd (e.g., Hamilton and others, 1978; Bennett
293 and others, 1993) and then zircon Lu-Hf (e.g., Hiess and others, 2009; Kemp and
294 others 2009; Amelin and others, 2011, Naerra and others, 2012) have supported this
295 fundamental finding, that is there is no isotopic evidence for the incorporation of
296 earlier Hadean felsic crust in the sources of the IGC orthogneisses.

297 Studies using whole rock Lu-Hf isotopic compositions of mafic, rocks rather
298 than zircons, from the ~3700 Ma and ~3800 Ma portions of the Isua supracrustal belt
299 further confirm this finding (Hoffmann and others, 2010, 2011b, Rizo and others
300 2011). For example, mica schists from the eastern end of the belt whose protoliths
301 were derived from the weathering of mafic volcanic rocks at ~ 3710 Ma (Nutman and
302 others, 1984a, 1997, 2009) and ~3720 Ma metabasalts all show a narrow range of near
303 -chondritic initial ϵ_{Hf} values between +2.5 to -0.7 (Fig. 6; Hoffmann and others 2010,
304 2011b). This suggests that they were the product of newly-formed mafic rocks, rather
305 than of a weathered Hadean protocrust (as was suggested by Kamber and others,
306 2005). Likewise, volcanosedimentary rocks from the western end of the belt (Rosing,
307 1999) with a depositional age of ~3710 Ma (Nutman and others, 2009) fall in the same
308 range of initial ϵ_{Hf} values (Fig. 6). An exception to the widespread near-chondritic
309 initial Hf isotopic compositions for mafic whole rocks and zircons for pre-3650 Ma
310 granitoids is seen in a suite of boninitic volcanic rocks (e.g. Polat and others, 2002).
311 This boninitic suite, with a likely age of ~3720 Ma, has a wide range of initial ϵ_{Hf}

312 values from +1 to >+10 (Fig. 6). Hoffmann and others (2010) explained this as due to
313 Eoarchean melting of a mantle reservoir that had fractionated Lu-Hf in the Hadean, in
314 order to evolve to the extreme positive ϵ_{Hf} values by ~3720 Ma. An alternative
315 explanation offered here is that these rocks represent partial melting of depleted upper
316 mantle containing entrained garnet \pm omphacite restite that resulted from early
317 Eoarchean tonalitic crust production. The extremely high Lu/Hf of such a source could
318 generate the highly positive ϵ_{Hf} values within ~200 hundred million years. Partial
319 melting in an olivine + garnet \pm omphacite source would also give rise to the
320 characteristic low Ca/Al ratios of these rocks.

321 Modelling of IGC whole rock Pb isotopic compositions has been used to
322 estimate the timing of crust separation from the mantle. However, in ancient gneiss
323 complexes such as the IGC, data from the same rocks can be used to reach contrasting
324 conclusions, ranging from large portions of the IGC having formed at ~3650 Ma
325 (Kamber and Moorbath, 1998), to earlier Eoarchean crust formation being important
326 (Tera, 2003), to derivation of some IGC rocks from a Hadean protocrust (Kamber and
327 others, 2003). Difficulties in interpreting this Pb data arise from the high mobility of
328 Pb coupled with fraction of Pb versus U (expressed as the μ value; $^{238}\text{U}/^{204}\text{Pb}$) in
329 tectonothermal events affecting the IGC (Baadsgaard and others, 1986b). Thus the Pb
330 isotopic data forms highly scattered arrays that intercept possible mantle growth curves
331 between ~3700-3600 Ma (e.g., Kamber and Moorbath, 1998; Kamber and others,
332 2003). Our preferred interpretation of these scatters is Pb-isotopic homogenization of
333 varying efficiency and modification of μ values during the Isukasian orogeny
334 (McGregor, 2000) and to a lesser degree in younger tectonothermal events. Support for
335 this comes from studies of much younger orogenic systems such as the Paleozoic
336 Lachan orogen of eastern Australia, where plutonic rocks derived from contrasting
337 crustal and mantle sources retain different and original whole rock Nd isotopic
338 signatures, whereas their Pb isotopic signatures have been homogenized (McCulloch
339 and Woodhead, 1993). Based on this and in consideration of increasing uncertainty
340 over appropriate U-Pb isotopic parameters for modelling the early Earth (e.g.
341 Albarede, 2009), we are cautious about suggestions based on scattered whole rock Pb
342 isotopic data that IGC rocks were derived from sources with input from Hadean
343 components (Kamber and others, 2003).

344 Thus using integrated U-Pb and Lu-Hf data from zircons and whole rock
345 Sm-Nd and Lu-Hf methods there is no compelling evidence within the IGC of Hadean
346 recycled ‘continental’ crust which would have resulted in strongly negative $\epsilon_{\text{Hf,Nd}}$
347 values by ~3900 Ma.

348

349 *Oceans before 3700 Ma*

350 Banded iron formation (BIF) is an early Precambrian chemical sedimentary
351 rock that precipitated in a marine environment thus providing evidence of a
352 hydrosphere early in Earth’s history. The first Pb-Pb whole rock dating at ≥ 3700 Ma of
353 Isua supracrustal belt BIF (Moorbath and others, 1973) showed that the hydrosphere
354 was established very early. This coupled with the recognition of pillow structures
355 within Isua supracrustal belt basalts (e.g., Komiya and others, 1999) means that for
356 surficial processes there was ‘normality’ within Earth’s first billion years, such as the
357 hydration and alteration of volcanic rocks. This means that recycling of mafic crust
358 back into the mantle at convergent plate boundaries could promote fluid-fluxing
359 melting as seen for the melting mechanism producing magmas in modern island arcs
360 (Polat and Hofmann, 2003; Dilek and Polat, 2009).

361

362 *Complex, protracted crustal evolution from the study of meta-plutonic rocks*

363 A bulk dissolution zircon U-Pb geochronological programme integrated with
364 whole rock Nd isotopic analysis on samples of single meta-igneous phases from IGC
365 low strain zones (Baadsgaard and others, 1986a) started to differentiate the age and
366 isotopic signatures of different plutonic protoliths in the IGC. This study was the first
367 to reveal a trend of increasingly less positive to negative initial ϵ_{Nd} , with a progression
368 from older juvenile tonalites to younger granites produced by crustal recycling.

369

370 *Isotopic signatures of multiple Eoarchean juvenile crustal components and* 371 *implications for early terrestrial differentiation*

372 By the mid 1990s, accumulated U-Pb zircon dates by SHRIMP showed that the
373 IGC contains several generations of tonalite suites, from ≥ 3850 Ma to ~3660 Ma
374 (Kinny, 1986; Nutman and others, 1993, 1996). Bennett and others (1993) obtained
375 initial $\epsilon_{\text{Nd}} > +2$ signatures of a sample subset of predominantly less
376 tectonothermally-reworked tonalite samples, showing that they were independent,

377 episodic extractions from a mantle with previous long-term depletion of Nd relative to
378 Sm. Both these findings have now been reproduced and accepted (e.g., Crowley and
379 others, 2002 and Crowley, 2003 for the zircon dating, and Caro and others, 2006 for
380 the whole rock Nd work). Further evidence for the juvenile nature of the tonalitic
381 orthogneisses comes from the mantle-like $^{18}\text{O}/^{16}\text{O}$ isotopic compositions of their
382 zircons as demonstrated by Hiess and others (2009) in the first *in situ* oxygen isotopic
383 study of zircons within the IGC.

384

385 *Eoarchean juvenile crustal igneous rocks have geochemical signatures resembling*
386 *ones formed at younger convergent plate boundaries*

387 Whole rock geochemical studies of non-migmatized tonalites showed they are
388 predominantly products of partial melting of eclogitized mafic rocks (Nutman et al.,
389 1999). Although the melting of mafic rocks at high pressure is the widely accepted
390 source for these rocks, detailed trace element studies by Hoffmann and others (2011a)
391 suggested that melting at lower pressures (high pressure granulite assemblages?) is
392 feasible for some compositions. Furthermore, the composition of the source is debated.
393 Nutman and others (1999) suggested that a MORB-like source could be dominant,
394 whereas Nagel and others (2012) suggested it is more likely that the source was akin to
395 Isua arc-like basalts. However, in our opinion, this issue is clouded by the
396 compositions used in modelling by Nagel and others (2012) not being the best
397 representatives of Isua arc-like basalts. Clearly, further studies are required to
398 investigate the likely source compositions, and how they might have changed with
399 time as the Eoarchean arc-like assemblages evolved.

400 The mafic and intermediate rocks associated with the tonalites display
401 signatures showing domination of upper mantle sources that melted due to fluxing
402 from fluids released from a 'subducted' slab (e.g., Polat and Hofmann, 2003; Jenner
403 and others, 2009). More detailed examination of the trace element geochemistry of
404 Isua mafic rocks indicates that although this mechanism is dominant, there may also be
405 a contribution from slab melts (Hoffmann and others, 2011b). Combined with the
406 juvenile isotopic signatures of these rocks, this suggests that IGC Eoarchean crust
407 formed at convergent plate boundaries, in an environment with some resemblance to
408 modern intra-oceanic arc settings (see summary by Dilek and Polat, 2009).

409

410 *Eoarchean assembly of unrelated juvenile crust domains*

411 Integrated structural and zircon U-Pb dating studies demonstrate that juvenile
412 components of the IGC evolved separately, prior to assembly and a 3660-3600 Ma
413 orogeny (Nutman and others, 1993, 1996). The most detailed information on this
414 comes from the Isua supracrustal belt environs, where it is demonstrated that by 3660
415 Ma a juvenile northern composite ~3700 Ma arc-like assemblage was juxtaposed
416 against an older complex dominated by ~3800 Ma rocks, also likely the product of an
417 arc system (Figs 3B and 5; Nutman and others, 1996, 2009; Crowley, 2003; Jenner and
418 others, 2009; Nutman and Friend, 2009). These findings indicate that lateral
419 lithospheric movements resulting from upper mantle convection were occurring in the
420 Eoarchean, with the further implication that upper mantle convection was an available
421 and likely important heat-loss mechanism for the early Earth.

422

423 *Differentiation of the mantle reservoir that spawned Itsaq Gneiss Complex juvenile*
424 *crust*

425 Increasing integration of accurate and precise U-Pb zircon dating with whole
426 rock ^{143}Nd , ^{142}Nd , zircon Hf and whole rock W isotopic signatures are refining the
427 timing and nature of fundamental terrestrial differentiation to events within the first 60
428 million years of Earth history (e.g., Caro and others, 2006; Bennett and others, 2007;
429 Hiess and others, 2009, Willbold and others, 2011, Rizo and others, 2012).
430 Furthermore, they reveal that although these events strongly fractionated Sm and Nd in
431 the upper mantle reservoir, in did not fractionate Lu from Hf to the same degree. This
432 gives rise to the characteristic initial whole rock ϵ_{Nd} of +4 to +2, positive ^{142}Nd
433 isotopic anomalies of $>+10$ p.p.m. compared to modern rocks and zircon ϵ_{Hf} of +1 to 0
434 for Eoarchean juvenile crust (Fig. 6; Bennett and others, 1993, 2007; Hiess and others,
435 2009; Kemp and others, 2009; Amelin and others, 2011).

436

437 **COMPLETE SHRIMP ZIRCON U-PB GEOCHRONOLOGICAL SURVEY:**
438 **SNAPSHOT OF ITSAQ GNEISS COMPLEX EARLY CRUSTAL EVOLUTION**

439 Starting from 1986, zircons from ~160 IGC meta-igneous samples have now
440 been dated by the SHRIMP U-Pb technique. Compston and others (1986)
441 demonstrated (with then unsurpassed precision and accuracy) that felsic schists along

442 the southern margin of the Isua supracrustal belt have an age of 3806 ± 2 Ma. In
443 retrospect, the lack of younger overgrowths on these zircons suggests that
444 superimposed metamorphic events were mild at this locality. Kinny (1986) obtained an
445 older protolith age of 3822 ± 10 Ma for a tonalitic gneiss south of Nuuk (sample
446 110999; Fig. 1), with metamorphic overgrowths dated at ~ 3630 Ma. Combined with
447 the ~ 3700 Ma bulk zircon ages for other tonalites published in the same year
448 (Baadsgaard and others, 1986a), these initial studies showed that rocks of considerably
449 different age are present in the complex, and that high temperature metamorphic
450 overprint was variable and could be dated accurately. Broader geochronological
451 appraisals published by Nutman and others (1993, 1996) expanded upon this, and
452 presented data to demonstrate that the IGC's rock record extended to >3850 Ma, i.e.,
453 significantly older than rocks in the Isua supracrustal belt. Furthermore, these studies
454 demonstrated that even the oldest (≥ 3800 Ma) tonalite components did not start to
455 develop significant zircon metamorphic overgrowths until 3650-3600 Ma, which gave
456 rise to a model of accumulation of juvenile crustal assemblages prior to ~ 3650 Ma
457 without significant regional metamorphism, followed by 3650-3600 Ma high
458 temperature orogeny (Nutman and others, 1993). The lesser amount of ID-TIMS
459 zircon U-Pb dating has confirmed the diverse ages for rocks in the IGC (e.g., Crowley
460 and others, 2002; Crowley, 2003; Amelin and others, 2011).

461 Since 2004 there has been a programme of reconnaissance dating of >100
462 samples using the Hiroshima University SHRIMP (e.g., Horie and others, 2010). This
463 programme is completed, with dating now covering the whole IGC, albeit with varying
464 density. In this reconnaissance programme, typically ~ 10 cathodoluminescence-guided
465 analyses were undertaken per sample, in order to fill-in geographic areas of
466 considerable extent previously devoid of any age determinations. Extra analyses were
467 undertaken only when 'interesting' samples were revealed in the reconnaissance. Most
468 significant of these was the discovery of a mildly migmatized 3891 ± 6 Ma tonalite in
469 the southeastern part of the IGC (sample G01/36 on Fig. 1; Hiess and others, 2009;
470 Horie and others, 2010).

471

472 THE 3660-3600 Ma ISUKASIAN OROGENY

473 The IGC contains contrasting crustal levels juxtaposed during a 3660-3600 Ma
474 orogeny (Fig. 3; Griffin and others, 1980; Nutman and others, 1996; Friend and
475 Nutman, 2005a). This orogeny is named here the *Isukasian*, after the geographic region

476 *Isukasia* at the northern end of the Itsaq Gneiss Complex where effects of this orogeny
477 are least modified by superimposed Neoproterozoic orogenic events. However, new
478 structural and textural observations presented here provide further insight into crustal
479 response during this event and help suggest its cause.

480

481 *Anatomy of deep crustal migmatites*

482 The rare domains of lower strain in the IGC south of line 'N' (Fig. 5) show that
483 the juvenile tonalitic protoliths are only locally well preserved (Nutman and others,
484 2000, 2007a,b). As a generality, these tonalites were reduced to palaeosome in
485 complex migmatites, whose granitic neosome was derived both from *in situ* anatexis
486 of the tonalites and from intrusions (Fig. 4A). These anatectic and intrusive events
487 have been equated with petrographic evidence for high grade Proterozoic
488 metamorphism up to granulite facies (McGregor and Mason 1977; Griffin and others,
489 1980; Friend and Nutman 2005a).

490 These migmatites were generally converted into banded gneisses by
491 superimposed younger Proterozoic deformation, to such an extent, that they can be
492 'laundered' into superficially homogeneous rocks (Nutman and others, 2000, 2004b;
493 Horie et al., 2010). However, the tracing of these banded gneisses into small low strain
494 zones demonstrates their complex early history with several different igneous phases
495 present. This is not a trivial observation, because it resolves divergent interpretations
496 of these gneisses that are possible, if based solely on *in situ* zircon U-Pb zircon
497 geochronology, without taking geological field observations into account. Thus taking
498 these gneisses superficially as single igneous phases, Whitehouse and others (1999)
499 interpreted them as ~3650 Ma rocks that carried abundant older inherited zircons,
500 whereas using field observations, Nutman and others (1996, 2000) interpreted them as
501 polyphase samples with Proterozoic igneous components differing in age by as much as
502 200 million years. Such a divergence of opinion upon the age of rocks has major
503 ramifications concerning the initial whole rock isotopic signatures of these rocks and
504 thereby the severity of fractionation in the earliest upper mantle reservoirs (Bennett
505 and others, 2007).

506 Where least modified by superimposed post-Ameralik dyke (i.e. ~3500 Ma)
507 deformation, the deep crustal migmatites have a broadly planar fabric that Ameralik
508 dykes always cut at a high angle. Evidence of this angular relationship is widespread in
509 the area of very low post-3500 Ma strain north of the Isua supracrustal belt (Fig. 5),

510 where pre-3500 Ma tectonic fabrics are gently inclined but are cut by non-deformed
511 sub-vertical Ameralik dykes. Thus with the reasonable assumption that the majority of
512 dikes were originally steeply inclined, this would permit that the migmatitic structures
513 were originally sub-horizontal. Moreover, upon the same outcrop, the least modified
514 migmatites show varying degrees of strain in the neosome (Fig. 4A). This is best
515 explained by heterogeneous pre-3500 Ma ductile deformation, with *in situ* neosome
516 production and injection coeval with ductile deformation. The proposed originally
517 sub-horizontal nature of migmatite banding is best accommodated in deep crustal
518 lateral flow (Sandiford, 1989), and the presence of anatectic melt between ~3660 -
519 3600 Ma associated with *punctuated* thermal maxima at 3642 ± 16 , 3621 ± 8 , 3599 ± 6
520 Ma as recorded by zircon growth in migmatites on Akilia island (Friend and Nutman,
521 2005a) would have greatly enhanced strain (Hollister and Crawford, 1986). Thus we
522 propose that these migmatites lay testament to extreme strain with melt-lubricated
523 lateral flow of the deep crust over a period of ~50 million years.

524 Units of 3640-3635 Ma (Baadsgaard, 1973; Nutman and others, 2000; Hiess
525 and others, 2011) Fe-rich augen granites, monzonites and ferrogabbros are a distinct
526 component of the part of the IGC south of Ameralik (Fig. 1; McGregor, 1973). These
527 are the product of hybridization of fractionated magmas derived from the mantle and
528 anatexis of the deep crust, and consequently resemble A-type / within-plate-granites
529 with high Nb, Zr, TiO₂ and P₂O₅ (Nutman and others, 1984b, 1996). These rocks, like
530 their host neosome-soaked migmatites, allay to an elevated geothermal gradient in the
531 deep crust being linked at least in part by the emplacement of mantle-derived melts.

532

533 *3660-3600 Ma structures and granite emplacement in ~3800 Ma tonalites south of the*
534 *Isua supracrustal belt*

535 South of the Isua supracrustal belt (Fig. 5) all Ameralik dykes carry
536 metamorphic hornblende, and locally garnet. Thus, the 3800 Ma rocks were
537 overprinted by Neoproterozoic lower to middle amphibolite facies metamorphism
538 (Nutman and others, 1996). This is also demonstrated by 2700-2600 Ma U-Pb titanite
539 ages from these 3800 Ma rocks (Crowley, 2003) and a ~2690 Ma U-Pb monazite age
540 on an Eoarchean pegmatite (Nutman and others, 2002b). The tonalites south of the Isua
541 supracrustal belt contain rare areas of very low total strain (Fig. 4D), with preservation
542 of weakly plagioclase-phyric igneous textures (Nutman and others, 1999). However,
543 even these rocks with the lowest superimposed strain have been thoroughly

544 recrystallized, and no igneous phases are preserved, apart from zircon. Thus even
545 where there is a plagioclase-phyric texture, the igneous plagioclase phenocrysts have
546 been pseudomorphed by subgrain mosaics (Fig. 4F), which finally recrystallized
547 during superimposed Neoproterozoic amphibolite facies metamorphism. Another feature
548 of the ~3800 Ma terrane for at least 10 km south of the Isua supracrustal belt is the lack
549 of pre-Ameralik dyke (>3500 Ma) *in situ* anatexis within the tonalites and although
550 3660-3600 Ma granites occur, they are volumetrically less than to the north of the belt
551 (Nutman and others, 1999; Crowley, 2003). These form discrete intrusions, with a
552 tendency to have been emplaced in and around active shear zones (Friend and others,
553 2002; Nutman and others, 2002b). The ~3800 Ma tonalites may display a
554 pre-Ameralik dyke cataclastic texture, albeit this has been recrystallized during
555 superimposed Neoproterozoic amphibolite facies metamorphism. The possible presence
556 of such a texture, the lack of *in situ* anatexis and the focussing of 3660-3600 Ma
557 granitic intrusions along active shear zones rather than being distributed through
558 migmatites all suggest that at 3660-3600 Ma, the ~3800 Ma domain on the south side
559 of the Isua supracrustal belt was at a higher, cooler crustal level than the migmatites
560 that are prevalent in the southern exposures of the IGC. Exact conditions are yet to be
561 resolved, but the presence of pre-Ameralik dyke cataclastic textures would suggest
562 sub-amphibolite facies conditions.

563

564 *3660-3600 Ma structures, fabrics and granite emplacement in ~3700 Ma tonalites*
565 *north of the Isua supracrustal belt*

566 North of the Isua supracrustal belt, ~3700 Ma tonalites display a range of
567 relationships with several generations of 3660-3600 Ma granites, and there is ductile to
568 brittle fabric development prior to intrusion of the Ameralik dykes. Crowley and others
569 (2002) presented field observations integrated with U-Pb zircon and titanite
570 geochronology of two localities to provide more detailed insight into the early tectonic
571 history. They demonstrated (i) that the host tonalites ranged from undeformed to
572 foliated (S1) and folded prior to intrusion of the oldest granites, (ii) that the Inaluk
573 dykes (a composite suite of mafic diorite and comagmatic granitic pegmatite; Nutman
574 and Bridgwater, 1986) were intruded at 3659 ± 2 Ma, prior to (iii) intrusion of more
575 voluminous granite sheets at 3644 ± 3 Ma, which they regarded as synchronous with
576 the development of a second fabric (S2). Close to the Isua supracrustal belt they

577 recognized further deformation of the tonalites and granite sheets to give a third
578 foliation (S3).

579 In this paper we contribute new information on the relationships between
580 successive generations of granite and pegmatite intrusions and the tectonothermal
581 evolution. In the north-central part of this area, relationships between the tonalites and
582 granites are least-modified by superimposed, but still pre-Ameralik dyke, deformation
583 (Nutman and Bridgwater, 1986; this area is indicated as 'lowest strain domain' in Fig.
584 5). These rocks are overall 'fresh' with widespread preservation of igneous textures
585 (Fig. 4B), and the tonalites locally have relicts of igneous plagioclase in phenocrysts,
586 and granites and pegmatites contain fresh alkali feldspar and relict igneous plagioclase.
587 The tonalites were intruded by the 3659 ± 2 Ma Inaluk dykes (Fig. 4B; Crowley and
588 others, 2002), prior to local *in situ* anatexis of the tonalites with production of the
589 earliest granites (Fig. 4C). Paleosome schlieren in these early granites are
590 ductilely-deformed into sigmoidal shapes, indicative of syn-magmatic extensional
591 deformation (Fig. 4C). The schlieric granites are cut by better-defined granite sheets
592 that occupy fracture networks whose geometry also indicates extensional deformation.
593 These are equated with the granites in the same area dated at 3649 ± 6 Ma by Nutman
594 and others (2000) and 3644 ± 3 Ma by Crowley and others (2002).

595 In an amphibolite pod within a belt of pegmatite with widely developed flaser
596 texture (sample locality G11/24 in Fig. 5) we have discovered a lower strain zone with
597 the relict high-pressure granulite facies assemblage garnet + clinopyroxene +
598 hornblende + plagioclase + quartz (Fig. 7A). Dehydration partial melting is the likely
599 process because exterior to the segregations the amphibolites do not contain garnet and
600 clinopyroxene. Consequently, this assemblage is considered to have formed with
601 garnet + clinopyroxene \pm hornblende in equilibrium with a trondhjemitic melt
602 (crystallized as plagioclase + quartz). Zoned magmatic zircons in this partial melt
603 segregation (sample G11/24) have been dated by the SHRIMP U-Pb method
604 (Appendix 1). Small equant and prismatic zircons are oscillatory-zoned, with partial
605 recrystallization to give homogeneous or sector-zoned domains (Fig. 7B). In both
606 varieties U and Th/U are generally low (mostly <100 ppm and always <0.01,
607 respectively). Most analyses yield close to concordant U-Pb ages, with $^{207}\text{Pb}/^{206}\text{Pb}$
608 ages mostly between 3700 and 3550 Ma (Fig. 7C; Appendix 1). In some cases
609 distinctions between genuine oscillatory zoned igneous zircon and various types of
610 recrystallized zircon is very subtle. If there was any doubt that the analytical sites were

611 composite (containing both igneous + recrystallization domains) they were not used in
612 age assessments. Using this conservative approach, 3658 ± 3 Ma was obtained for the
613 oscillatory-zoned zircon, and 3635 ± 2 Ma and 3591 ± 5 Ma (all 95% confidence and
614 $MSWD \leq 1.0$) for successive generations of recrystallized zircon. Some other sites of
615 recrystallization occur in the centers of grains, are bright in CL images and have lost U
616 and Th (Fig. 7B). Some of these sites have markedly reverse discordant ages, coupled
617 with older $^{207}\text{Pb}/^{206}\text{Pb}$ ages, suggesting non-supported radiogenic Pb. 3658 ± 3 Ma is
618 indistinguishable from the Crowley and others (2002) 3659 ± 2 Ma age obtained on the
619 Inaluk dykes, the first event *common* to both the northern ~ 3700 Ma and southern
620 ~ 3800 Ma terranes. This ties the elevated pressure event to the *start* of the common
621 history between the two terranes. Reconstruction of the pressure-temperature-time
622 history of this sample will be reported elsewhere, but preliminary estimates indicate
623 pressures of ≥ 1 GPa. The sample G11/24 zircon recrystallization age of 3635 ± 2 Ma
624 agrees with the age of 3633 ± 5 obtained on a flaser pegmatite strand in the central
625 gneisses (Nutman et al., 2002b). 3591 ± 5 Ma agrees with zircon recrystallization ages
626 previously obtained from the Isua area (Nutman et al., 2002b).

627 Away from the area of ‘freshest’ rocks indicated as ‘lowest strain domain’ in
628 Figure 5, both the tonalites and cross-cutting granites have been variably and locally
629 strongly deformed prior to intrusion of the Ameralik dykes (Nutman, 1984; Crowley
630 and others, 2002). This has locally reduced the granite sheets to subconcordant layers
631 within their tonalite host. Well north of the Isua supracrustal belt, in areas devoid of
632 post-Ameralik dyke strain (i.e., the dikes are close to vertical and non-deformed),
633 cataclastic texture is preserved within such rocks (Fig. 4F), with kinematic indicators
634 indicating extensional deformation. This pre-Ameralik dyke cataclastic texture
635 indicates Eoarchean deformation at the ductile-brittle transition, under
636 sub-amphibolite facies conditions. Micro-fabrics related to this are indicated in Fig.
637 4G, with ribbon quartz and the degradation of plagioclase into altered subgrains
638 defining the S fabric. Note that fine-grained biotite grains are randomly orientated
639 across this fabric, having grown during superimposed ‘static’ Neoproterozoic
640 epidote-amphibolite facies metamorphism. The development of the cataclastic
641 textures is synchronous with, or predates, the intrusion of strands of syn-kinematic
642 3640-3630 Ma flaser-textured pegmatite. The strands of flaser-textured pegmatite are
643 continuous for many kilometres and contain trains of ultramafic, amphibolite and
644 siliceous inclusions. These inclusions are probably dismembered supracrustal rocks,

645 and seem largely restricted to the shear zones occupied by the pegmatites (Nutman,
646 1984; Nutman and Friend, 2009).

647 Thus the gneiss complex north of the Isua supracrustal belt shows a 3650 Ma to
648 ~3630 Ma record of repeated granite emplacement that started at deeper high
649 temperature domains with the development of schlieric migmatites (Fig. 4C) following
650 on from transient high-pressure metamorphism (sample G11/24), through the
651 emplacement of granites as sheets occupying fractures (but where ductile deformation
652 could be sustained at lower strain rates), to emplacement synchronous or post-dating
653 sub-amphibolite facies cataclasis (Fig. 4F). In all cases there are structural indications
654 of extensional deformation. Extension over the course of ≥ 10 million years gave rise to
655 tectonic thinning of the crust, and might be responsible for elevating the host rocks
656 from the fringes of the ductile anatectic zone ($\geq 650^\circ\text{C}$?) to cataclastic sub-amphibolite
657 facies conditions ($< 500^\circ\text{C}$). This can explain the telescoping of early metamorphic
658 conditions in the Isua area from greenschist / epidote amphibolite facies to upper
659 amphibolite facies migmatites, with ‘jumps’ of early metamorphic grade across
660 Eoarchean shear zones (Fig. 3B).

661

662

3660-3600 Ma shear zones

663 In the Isua area, the juvenile crustal components are partitioned by
664 pre-Ameralik dyke (> 3500 Ma) shear zones (Nutman, 1984; Nutman and Friend,
665 2009). One of these shear zones defines the eastern-central margin of the Isua
666 supracrustal belt, but westwards cuts into the belt (Fig. 5; Nutman and Friend, 2009).
667 This shear zone post-dates 3649 ± 4 Ma granite sheets (Crowley and others, 2002). At
668 the margin of the Isua supracrustal belt this shear zone is commonly occupied by
669 syn-kinematic flaser-textured pegmatite (Nutman, 1984). Constraining the age of shear
670 zones south of the belt are U-Pb zircon 3645 ± 7 Ma and 3607 ± 5 Ma ages for pre- and
671 post-mylonite granite sheets (Friend and others, 2002; Nutman and others, 2002b) and
672 for north of the belt a 3633 ± 7 Ma syn-mylonite pegmatite (Nutman and others,
673 2002b).

674

675

DISCUSSION

676

Mosaic of ages across the Itsaq Gneiss Complex

677 There is a mosaic of different ‘families’ of tonalite protolith ages with each
678 ‘family’ containing two or more ‘generations’ (Fig. 2). The youngest at ~3660 Ma

679 (Friend and Nutman, 2005a) forms a limited <5 km broad domain around Amittsoq
680 (McGregor's type locality for the Amittsoq gneisses; Fig. 1). These are devoid of the
681 strong Eoarchean tectonothermal overprint; anatexis is only seen in older Eoarchean
682 rocks flanking both sides of the Amittsoq domain, with which they appear to be
683 tectonically juxtaposed (Friend and Nutman, 2005a). Tonalites with ages of ~3800 Ma
684 form another family, which comprises 3820-3805 and 3795-3790 Ma generations.
685 South of the Isua supracrustal belt to beyond line 'N' these form a uniform assemblage,
686 apparently devoid of older components (Fig. 5; Nutman and others, 1999, 2002b;
687 Crowley, 2003). On Akilia and several surrounding islands, at the northern edge of the
688 Mesoarchean Ivisartoq supracrustal belt, and in the southeastern part of the IGC in
689 Itilleq (Fig. 1), a 3890-3840 Ma tonalite family has been detected (Nutman and others,
690 1996, 1997b, 2000, 2002a, 2007b; Hiess and others, 2009; Horie and others, 2010).
691 Commonly associated with them are ~3760 Ma tonalites. Local low strain zones
692 preserve evidence that the ≥ 3840 Ma rocks were intruded by ~3760 Ma tonalites
693 (Nutman and others, 2000), but the relationships with nearby ~3800 Ma rocks is
694 presently unknown. The ~3700 Ma tonalite family (with 3715-3710 and 3700-3685
695 Ma generations) is best preserved to the north of the Isua supracrustal belt, where they
696 are found in tectonic contact with ~3800 Ma rocks to the south (Fig. 5). Migmatized
697 ~3700 Ma tonalites form other parts of the IGC. For example at the southeastern edge
698 of the IGC in Itilleq and Ameralla (Fig. 1), migmatites with ~3700 Ma paleosome
699 appear to be mutually exclusive from domains with ≥ 3800 Ma paleosome (Horie and
700 others, 2010). Thus despite the strong superimposed Neoproterozoic deformation in this
701 part of the IGC, it is possible that different ~3700 Ma and ≥ 3800 Ma tonalitic units
702 were also tectonically assembled, prior to a common 3660-3600 Ma migmatization
703 event.

704 The accrued dating program also permits oversight on the extent of 3660-3600
705 Ma new zircon overgrowths in the juvenile tonalites. In a broad fashion, this is a proxy
706 of 3660-3600 Ma high metamorphic temperatures. This is a valid assumption, because
707 in the migmatites in the south of the complex, zircons were most modified at
708 3660-3600 Ma, the rocks are most intensely migmatized, and they preserve local
709 relicts of Eoarchean granulite facies metamorphism (Nutman and others, 2000, 2002a;
710 Friend and Nutman, 2005a). The widespread occurrence of 3660-3600 Ma
711 overgrowths indicates that much of the IGC was affected by high temperatures at that
712 time, with the significant exception being parts of northern end of the IGC around the

713 Isua supracrustal belt, and other small (tectonically bounded?) domains such as around
714 Amiiitsoq in Ameralik. The recent SHRIMP and IDTIMS U-Pb zircon ages of IGC
715 granites (e.g. Nutman and others, 1993, 1996, 2000; Crowley and others, 2002)
716 confirms Baadsgaard and others (1986a) observations that they all have ages of ≤ 3660
717 Ma and are related to high temperatures in an orogeny that reworked the older juvenile
718 crust dominated by tonalites.

719 Finally, the dating program has largely confirmed the extent of the IGC, as
720 originally defined using its lithological characteristics by McGregor (1973); that these
721 rocks are cut by deformed, amphibolitized mafic dikes. A few exceptions to this have
722 been found (Kinny, 1987; Schiøtte and others, 1989b) where in the 1970s some rocks
723 designated in the field as Eoarchean were discovered from U-Pb zircon dating to be
724 Neoproterozoic in age. The relevant localities are marked in Figure 1 by red circles.
725 Overall, these have reduced the extent of the IGC by $<5\%$.

726 In order to put all this information in an accessible format it is presented in five
727 histograms backed by relative frequency distribution curves (Fig. 8)². Figure 8A shows
728 the tonalite juvenile components from those parts of the IGC with the least
729 migmatization during the 3660-3600 Ma Isukasian orogeny. Note the clear distinction
730 of oscillatory-zoned zircon giving tonalite ages at ≥ 3850 Ma (subordinate), 3800 Ma
731 and 3700 Ma. The smear of ages down to ~ 3600 Ma is minimal, and this agrees with
732 field observations that these rocks generally show only minor migmatization. Figure
733 8B shows strongly migmatized juvenile tonalitic components throughout the
734 remaining parts of the IGC. Note here that although the same age peaks are apparent,
735 plus a minor one at ~ 3760 Ma, they are much less well defined, with a larger
736 proportion of ages falling between 3660-3600 Ma. This is accounted for by
737 recrystallization and partial ancient loss of radiogenic Pb from the protolith zircons.
738 Thus recrystallized/disturbed ~ 3850 Ma protolith zircons will present a smear of
739 apparent ages from 3850 to 3600 Ma, likewise similarly-affected ~ 3700 Ma protolith
740 zircons will present a smear of apparent ages from 3700 to 3600 Ma. This is in accord
741 with the complex nature of these migmatites, and structurally complex zircons within
742 them that display much regrowth and recrystallization (e.g., Nutman and others, 2000;
743 Horie and others, 2010). Figures 8C and 8D show the ages of zircons from granites
744 exterior to and within shear zones, in the least-migmatized parts of the IGC. Note all

745 granites formed post-3660 Ma, and that they carry only rare inherited zircon. Figure 8E
746 shows ages of zircons from granites and coeval gabbros in formerly deep, migmatitic,
747 parts of the IGC. Note that more than one age of intrusion is apparent, but there is a
748 close match in ages with granites dated from non-migmatized parts of the IGC.

749

750 *Juvenile crust formation – Eoarchean island arcs?*

751 Information from the different-aged juvenile assemblages in the IGC,
752 particularly the ~3700 Ma portion of the Isua supracrustal belt, chart out a history of
753 crustal development with similarities to Phanerozoic crustal processes. Thus Isua
754 juvenile 3720-3710 Ma crust development was initially by boninite, tholeiite and
755 picrite eruption, with mafic tonalite and quartz-diorite intrusion (Polat and Hofmann,
756 2003; Nutman and others, 2007; Friend and Nutman, 2010), but between 3710-3700
757 Ma had evolved to maturity with formation of andesites, dacites, related sediments,
758 and finally at 3700-3690 Ma emplacement of tonalites and granodiorites (Nutman and
759 others, 1996, 1997a, 2000, 2002, 2007a, 2009; Crowley et al., 2002; Bohlar et al.,
760 2005). The geochemical signatures of this assemblage of igneous rocks indicate
761 magma generation for the mafic-intermediate suites by hydrous fluxing of the upper
762 mantle and melting of eclogitized mafic crust for the quartzo-feldspathic suites (e.g.,
763 Nutman and others, 1999; Polat and Hofmann, 2003; Dilek and Polat, 2009; Jenner
764 and others, 2009; Nagel and others, 2012). This, combined with the age progression of
765 different lithologies, the tectonic insertion of mantle dunite slivers by 3710 Ma (Friend
766 and Nutman, 2011) and the juvenile isotopic signatures (e.g., Moorbath and others,
767 1972; Bennett and others 1993; Hiess and others, 2009) all point to a strong
768 resemblance with the sequence of rocks observed during development of intra-oceanic
769 arc complexes (alternatively known as suprasubduction zone ophiolites; Shervais,
770 2001). Therefore we conclude that this is their most likely environment of formation.
771 However, despite its lithological association, the 3720-3690 Ma assemblage is not an
772 intact section through a suprasubduction ophiolite, because, for example, convincing
773 ‘sheeted dike’ complexes have not been found (Friend and Nutman, 2010) and this
774 assemblage was repeatedly partitioned by Eoarchean shear zones (Nutman and Friend,
775 2009).

² Data have been subjected to filters of $f_{206} < 2\%$ (where f_{206} is the proportion of ^{206}Pb not of in situ uranium origin, based of measured ^{204}Pb and Cumming & Richards (1975) model common Pb compositions) and differences in the $^{207}\text{Pb}/^{206}\text{Pb}$ and $^{206}\text{Pb}/^{238}\text{U}$ ages of $<10\%$, i.e., $<10\%$ discordant.

776 The 3720-3690 Ma juvenile assemblage was juxtaposed to the south with a
777 3800 Ma complex, and hence it resembles Sierran-style ophiolites that are ensimatic
778 island arc terranes accreted against older crust (Shervais, 2001 and references therein).
779 This supports continuity of crust-formation processes at convergent plate boundaries
780 for almost 4 billion years. The pattern of ages and lithological types in the rest of the
781 IGC provide further evidence that this interpretation of crust formation was
782 appropriate for all juvenile components from at least 3890 to 3660 Ma, although
783 superimposed 3660-3600 Ma and Neoproterozoic orogenies have destroyed most the field
784 evidence that would support (or refute!) this contention.

785

786

Contrasting crustal levels at 3660-3600 Ma

787 The migmatites that dominate most of the IGC hold a record of sustained high
788 temperatures at moderate pressures throughout the 3660-3600 Ma Isukasian orogeny
789 (Friend and Nutman, 2005a). The ~3700 Ma tonalite terrane north of the Isua
790 supracrustal belt shows evidence of hot (and deep) crustal conditions and ductile
791 deformation at the start of the 3660-3600 Ma period, with a transition to cooler (and
792 shallower?) conditions, with brittle failure, at the end of the period. The ~3800 Ma tonalite
793 terrane south of the Isua supracrustal belt appears to show only cooler (shallow?)
794 crustal conditions throughout this period.

795

796

797

798

799

800

801

802

803

804

805

806

807

808

809

In the Isua area, shear zones partition the products of juvenile crust production. Movements on these shear zones have been constrained to between 3645-3607 Ma, by the ages of pre- syn- and post-kinematic granite and pegmatite sheets involved with them (Crowley and others, 2002; Friend and others, 2002; Nutman and others, 2002b; data in this paper). These shear zones combined with increasing evidence for extensional deformation, might be responsible for telescoping portions of the crust that resided in the deep, hot, ductile regime against those from a shallower cooler brittle regime (Fig. 3B). New evidence for this comes from the ~3700 Ma tonalite complex north of the Isua supracrustal belt, which at ~3650 Ma was in a hot ductile regime with incipient migmatization (Fig. 4C) but by 3600 Ma had been transferred to a cooler regime with deformation by cataclasis (Fig. 4F). Titanite U-Pb dates of 3606 ± 3 Ma (from a 3659 Ma Inaluk dyke), 3606 ± 3 Ma (from a 3698 ± 2 Ma tonalite) and 3603 ± 3 Ma (from a ~3645 Ma granite; Crowley and others, 2002) are in accord with this interpretation.

810 *The nature of the 3660-3600 Ma Isukasian orogeny*

811 The whole of the IGC was affected by the Isukasian orogeny. Thus the Isukasian
812 orogen covered a larger expanse of Eoarchean ‘continental’ crust than just the IGC,
813 with this larger crustal mass being fragmented and dispersed starting from ~3500 Ma,
814 as marked by intrusion of the Ameralik dykes. This is analogous to the way that on
815 either side of the South Atlantic there is Precambrian crust affected by the
816 Neoproterozoic Brasiliano orogen in South America and the Pan African orogen in
817 Africa – these being dispersed fragments of continental crust affected by a larger
818 orogenic system.

819 Understanding the geodynamic framework of the Isukasian orogen is impeded
820 not only by fragmentation, but also because its surviving pieces have only small areas
821 that were not reworked in superimposed post-3500 Ma orogenic events (Nutman and
822 others, 1996). Furthermore, thermo-mechanical modelling (e.g., Duclaux and others,
823 2007; Rey and Coltice, 2008) shows the much greater heat production from
824 radionuclides in the Archean than today means that compared with modern collisional
825 orogens, tectonically thickened crust in the Eoarchean had greater propensity to
826 undergo deep crustal anatexis and collapse. The greater degree of partial melting made
827 the Eoarchean deep crust very mobile and thereby destroyed much of the evidence on
828 the mechanism of previous crustal thickening (Figs 3C, 4A). This is significant
829 handicap, because most of the surviving IGC was in the deep crust during the Isukasian
830 orogeny. Notwithstanding, models to explain the Isukasian orogeny must account for
831 the following:

832 (1) It was a sustained event lasting for ~50 million years, as shown by 3660-3610 Ma
833 zircon ages on migmatization and granite bodies (Fig. 8C-E), followed by U-Pb
834 closure of the titanite at ~3605 Ma³ (e.g., Nutman and others, 2000; Crowley and
835 others, 2002; Friend and Nutman 2005a; Friend and others, 2002).

836 (2) There is mounting evidence suggesting extensional deformation was important
837 during the orogeny; (i) at middle-upper crustal levels granite sheets were emplaced
838 into extensional fractures; (ii) a major Eoarchean shear zone in the eastern end of the
839 Isua supracrustal belt has kyanite-bearing upper amphibolite facies rocks in the
840 footwall and greenschist to epidote-amphibolite rocks in the hangingwall (Fig. 3B) and

³ This key piece of information has been obliterated from most of the Itsaq Gneiss Complex by superimposed tectonothermal events, but survives in the plutonic complex of c. 3700 Ma tonalites and granite sheets north of the Isua supracrustal belt.

841 (iii) in the melt-lubricated deep crustal migmatites, 3640 Ma composite granite-gabbro
842 intrusions show syn-magmatic extensional features (Fig. 4H).

843 (3) The event followed on from ≥ 3900 to 3660 Ma juvenile crustal growth without
844 high temperature metamorphism (Nutman and others, 1993; Bennett and others,
845 1993). This appears to have been terminated by the start of the orogeny, with transient
846 high-pressure metamorphism (newly-discovered high pressure granulite – see above)
847 and then a switchover to crustal recycling marked by an elevated geothermal gradient
848 and deep crustal melting at moderate pressures (Friend and Nutman, 2005a).

849 Thus modern analogs must involve crustal reworking following assembly of
850 unrelated terranes, with protracted high heat flow taking place in an overall extensional
851 regime. A possible analog is continental northeast Asia, which following final early
852 Mesozoic assembly of arc terranes and older continental blocks has suffered
853 quasi-continuous extension up to the present time. This has caused extensive crustal
854 thinning, with the widespread development of core complexes, particularly in the
855 Cretaceous (e.g., Ren and others, 2002; Yang and others, 2007). Extension has been to
856 the extent that the underlying lithospheric mantle has been largely removed (e.g., Fan
857 and others, 2000). There is still debate concerning the cause of this high heat flow
858 extensional regime. However, one potential control is the continual eastward roll-back
859 of subduction systems into the northern Pacific, promoting behind it continued
860 extension of continental northeastern Asia (e.g., Wei and others, 2012 and references
861 therein).

862 In reality, establishing the geodynamic setting of the Isukasian orogeny is
863 hampered by the small size of the IGC – in the modern context it would be hard to
864 establish the geodynamic setting of the entire Himalayan - European Alps system
865 based on only 3000 km² of amphibolite facies tectonites!

866

867

CONCLUSIONS

868 (1) Four decades of research with increasingly sophisticated isotopic analytical
869 techniques all indicate that Eoarchean crust embodied by the Itsaq Gneiss Complex
870 was extracted from a depleted upper mantle reservoir in the Eoarchean; i.e. it was
871 juvenile at that time and not formed from recycled Hadean material.

872 (2) The accrued zircon U-Pb geochronology shows that juvenile crustal components
873 are not a single generation, but formed in several episodes from ~3900 to ~3660 Ma.

874 (3) Juvenile crust domains of different age are mutually exclusive, and evidence from
875 around the Isua supracrustal belt shows that they were tectonically assembled by 3660
876 Ma. This indicates that the crust grew by lateral accretion.

877 (4) The geochemistry of the juvenile Eoarchean igneous rocks points to derivation by
878 partial melting of eclogitized (and maybe also high pressure granulite) mafic rocks and
879 fluid-fluxing of upper mantle peridotite. This suggests these rocks formed at
880 convergent plate boundaries in environments akin to modern suprasubduction zone
881 settings. The detailed chronology obtained on the ~3700 Ma portion of the Isua
882 supracrustal belt shows a mafic to felsic progression from 3720-3710 Ma
883 basalts/gabbros, 3710-3700 Ma andesites/diorites to ~3690 Ma tonalites, and suggests
884 these rocks are samples of arcs evolving over a time span of 10-25 million years.

885 (5) Within the extent of the present Itsaq Gneiss Complex, juvenile crust production
886 ceased at ~3660 Ma, and was followed by the Isukasian orogeny which lasted to 3600
887 Ma. The isotopic signatures of 3650-3600 Ma granites formed during the Isukasian
888 orogeny demonstrate that they were at least partially derived from slightly older,
889 isotopically evolved, crustal components. The hallmark of this orogeny was elevated
890 heat flow with migmatization of much of the lower crust, and granite emplacement at
891 higher levels. There is increasing structural evidence for extensional deformation
892 being prevalent after inception of the orogen.

893 (6) Given (i) the overall small size of the Itsaq Gneiss Complex, (ii) the even smaller
894 area in it where structures relating to the 3660-3600 Ma orogen are preserved, and (iii)
895 that it represents just a fragment of the larger Isukasian orogen, it is not yet possible to
896 identify with certainty the broader geodynamic setting of the orogen. A possible
897 scenario for further exploration is extension following northeastern Asian-style early
898 Mesozoic terrane assembly and subsequent Pacific-ward eastward migration of
899 subduction systems.

900 (7) The accrued body of knowledge from the Itsaq Gneiss Complex shows that
901 Eoarchean crust-forming events and orogeny had strong similarities with processes
902 operating in the Phanerozoic, and indicate that some form of plate tectonics operated
903 almost 4 billion years ago.

904
905

ACKNOWLEDGEMENTS

906 We thank J. E. Hoffman, P. Cawood and editor S. Wilde for their constructive and thoughtful
907 reviews. Research on the Itsaq Gneiss Complex was supported by NERC grant

908 NER/A/S/1999/00024, ARC grants DP0342798, DP110104981, the Korean Basic Science
909 Institute, the University of Wollongong GeoQuEST Research Centre and Hiroshima
910 University.
911

912 REFERENCES

- 913 Albaréde, F., 2009, Volatile accretion history of the terrestrial planets and dynamic
914 implications: *Nature*, v. 461, p.1227-1233.
- 915 Allaart, J. H., 1976, The pre-3760 m.y. old supracrustal rocks of the Isua area, central West
916 Greenland, and the associated occurrence of quartz-banded ironstone: In: Windley,
917 B.F. (ed), *The Early History of the Earth*. Wiley, London, pp. 177-189.
- 918 Amelin, Y., Kamo, S. L., and Lee, D. C., 2011, Evolution of early crust in chondritic or
919 non-chondritic Earth inferred from U-Pb and Lu-Hf data for chemically abraded zircon
920 from the Itsaq Gneiss Complex, West Greenland: *Canadian Journal of Earth Sciences*,
921 v. 48, p. 141-160, doi: 10.1139/E10-091.
- 922 Baadsgaard, H., 1973, U-Th-Pb dates on zircons from the early Precambrian Amîtsoq
923 gneisses, Godthaab district, West Greenland: *Earth and Planetary Science Letters*, v.
924 19, p. 22-28.
- 925 Baadsgaard, H., Nutman, A. P., and Bridgwater, D., 1986a, Geochronology and isotope
926 geochemistry of the early Archaean Amîtsoq gneisses of the Isukasia area, southern
927 West Greenland: *Geochimica et Cosmochimica Acta*, v. 50, p. 2173-2183.
- 928 Baadsgaard, H., Nutman, A. P., Rosing, M., Brisgwater, D., and Longstaffe, F.J., 1986b,
929 Alteration and metamorphism of Amîtsoq gneisses from the Isukasia area, West
930 Greenland: Recommendation for isotope studies of the early crust: *Geochimica et*
931 *Cosmochimica Acta*, v. 50, p. 2165-2172.
- 932 Bennett, V. C., Nutman, A. P., and McCulloch, M. T., 1993, Nd isotopic evidence for
933 transient, highly depleted mantle reservoirs in the early history of the Earth: *Earth and*
934 *Planetary Science Letters*, v. 119, p. 299-317.
- 935 Bennett, V. C., Nutman, A. P., and Esat, T. M., 2003, Constraints on mantle evolution and
936 differentiation from $^{187}\text{Os}/^{188}\text{Os}$ isotopic compositions of Archaean ultramafic rocks
937 from southern West Greenland (3.8 Ga) and Western Australia (3.45 Ga): *Geochimica*
938 *et Cosmochimica Acta*, v. 66, p. 2615-2630.
- 939 Bennett V. C., Brandon, A. D., and Nutman, A. P., 2007, Hadean mantle dynamics from
940 coupled 142-143 neodymium isotopes in Eoarchaeon rocks: *Science*, v. 318, p.
941 1907-1910.
- 942 Black, L. P., Gale, N. H., Moorbath, S., Pankhurst, R. J., and McGregor, V. R., 1971, Isotopic
943 dating of very early Precambrian amphibolite facies gneisses from the Godthåb district,
944 West Greenland: *Earth and Planetary Science Letters*, v. 12, p. 245-259.

- 945 Bohlar, R., Kamber, B. S., Moorbath, S., Fedo, C. M., and Whitehouse, M. J., 2004,
946 Characterisation of early Archaean chemical sediments by trace element signatures:
947 Earth and Planetary Science Letters, v. 222, p. 43-60.
- 948 Bohlar, R., Kamber, B. S., Moorbath, S., Whitehouse, M. J., and Collerson, K. D.,
949 2005, Chemical characterization of earth's most ancient clastic metasediments
950 from Isua: *Geochimica et Cosmochimica Acta*, v. 69, p. 1553–1573.
- 951 Bowring, S., and Williams, I. S., 1999, Priscoan (4.00-4.03 Ga) orthogneisses from
952 northwestern Canada: *Contributions to Mineralogy and Petrology*, v. 134, p.
953 3-16.
- 954 Bridgwater, D., and McGregor, V. R., 1974, Field work on the very early Precambrian
955 rocks of the Isua area, southern West Greenland: *Rapport Grønlands Geologiske*
956 *Undersøgelse*, v. 65, p. 49-54.
- 957 Caro, G., Bourdon, B., Birk, J-L., and Moorbath, S., 2006, High-precision $^{142}\text{Nd}/^{144}\text{Nd}$
958 measurements in terrestrial rocks: Constraints on the early differentiation of Earth's
959 mantle: *Geochimica et Cosmochimica Acta*, v. 70, p. 164-191.
- 960 Chadwick, B., and Crewe, M. A., 1986, Chromite in the early Archaean Akilia association (c.
961 3,800 m.y.), Ivisârtoq region, inner Godthåbsfjord, southern West Greenland:
962 *Economic Geology*, v. 81, p. 184-191.
- 963 Compston, W., Kinny, P. D., Williams, I. S., and Foster, J. J., 1986, The age and lead loss
964 behaviour of zircons from the Isua supracrustal belt as determined by ion microprobe:
965 *Earth and Planetary Science Letters*, v. 80, p. 71-81.
- 966 Craddock, P. R., and Dauphas, N., 2011, Iron and carbon isotope evidence for microbial iron
967 respiration throughout the Archean: *Earth and Planetary Science Letters*, v. 303, p.
968 121–132.
- 969 Crowley, J. L., 2002, Testing the model of late Archean terrane accretion in southern West
970 Greenland: a comparison of timing of geological events across the Qarliit Nunaat fault,
971 Buksefjorden region: *Precambrian Research*, v. 116, p. 57-79.
- 972 Crowley, J. L., 2003, U-Pb geochronology of 3810-3630 Ma granitoid rocks south of the Isua
973 greenstone belt, southern West Greenland: *Precambrian Research*, v. 126, p. 235-257.
- 974 Crowley, J. L., Myers, J. S., and Dunning, G. R., 2002, The timing and nature of multiple
975 3700-3600 Ma tectonic events in granitoid rocks north of the Isua greenstone belt,
976 southern West Greenland: *Geological Society of America Bulletin*, v. 114, p.
977 1311-1325.
- 978 Cumming, G. L., and Richards, J. R., 1975, Ore lead ratios in a continuously changing Earth:
979 *Earth and Planetary Science Letters*, v. 28, p. 155-171.
- 980 Dilek, Y., and Polat, A., 2008, Suprasubduction zone ophiolites and Archean tectonics:
981 *Geology*, v. 36, p. 431–432, doi:10.1130/Focus052008.1.

- 982 Dauphas, N., Van Zuilen, M., Wadhwa, M., Davis, A. M., Marty, B., and Janney, P. E., 2004,
983 Clues from Fe isotope variations on the origin of early Archean BIFs from Greenland:
984 Science, v. 306, p. 2077-2080.
- 985 Duclaux, G., Rey, P., and Ménot, R. P., 2007, Orogen-parallel flow during continental
986 convergence: Numerical experiments and Archaean field examples: Geology, v.
987 35, p. 715-718.
- 988 Dymek, R. F., Brothers, S. C., and Schiffries, C. M., 1988, Petrogenesis of ultramafic
989 metamorphic rocks from the 3800 Ma Isua supracrustal belt, West Greenland:
990 Journal of Petrology, v. 29, p. 1353-1397.
- 991 Dymek, R. F., and Klein, C., 1988, Chemistry, petrology and origin of banded iron-formation
992 lithologies from the 3800 Ma Isua supracrustal belt, West Greenland: Precambrian
993 Research, v. 37, p. 247-302.
- 994 Fan, W. M., Zhang, H. F., Baker, J., Jarvis, K. E., Mason, P. R. D., and Menzies, M., 2000,
995 On and off the North China Craton: Where is the Archaean keel?: Journal of Petrology,
996 v. 41, p. 933-950.
- 997 Friend, C. R. L., and Nutman, A. P., 2005a, Complex 3670-3500 Ma orogenic episodes
998 superimposed on juvenile crust accreted between 3850-3690 Ma, Itsaq Gneiss
999 Complex, southern West Greenland: Journal of Geology, v. 113, p. 375-398.
- 1000 Friend, C. R. L., and Nutman, A. P., 2005b, New pieces to the Archaean terrane jigsaw puzzle
1001 in the Nuuk region, southern West Greenland: Steps in transforming a simple insight
1002 into a complex regional tectonothermal model: Journal of the Geological Society,
1003 London, v. 162, p. 147-163.
- 1004 Friend, C. R. L., and Nutman, A. P., 2010, Eoarchean ophiolites? New evidence for the
1005 debate on the Isua supracrustal belt, southern West Greenland: American Journal of
1006 Science, v. 310, p. 826-861.
- 1007 Friend, C. R. L., and Nutman, A. P., 2011, Dunites from Isua, southern West Greenland: A
1008 ca. 3720 Ma window into subcrustal metasomatism of depleted mantle: Geology, v. 39,
1009 p. 663-666.
- 1010 Friend, C. R. L., Bennett, V. C., and Nutman, A. P., 2002, Abyssal peridotites >3,800 Ma
1011 from southern West Greenland: field relationships, petrography, geochronology,
1012 whole-rock and mineral chemistry of dunite and harzburgite inclusions in the Itsaq
1013 Gneiss Complex: Contributions to Mineralogy and Petrology, v. 143, p. 71-92.
- 1014 Friend, C. R. L., Nutman, A. P., and McGregor, V. R., 1987, Late-Archaean tectonics in the
1015 Færingehavn - Tre Brødre area, south of Buksefjorden, southern West Greenland:
1016 Journal of the Geological Society, London, v. 144, p. 369-376.
- 1017 Friend, C. R. L., Bennett, V. C., Nutman, A. P., and Norman, M. D., 2007, Seawater trace
1018 element signatures (REE+Y) from Eoarchean chemical (meta)sedimentary rocks,
1019 southern West Greenland: Contributions to Mineralogy and Petrology, xxx, yyy-zzz,
1020 DOI 10.1007/S00410-007-0239-z.

- 1021 Friend, C. R. L., Nutman, A. P., and McGregor, V.R., 1988, Late Archaean terrane accretion
1022 in the Godthåb region, southern West Greenland: *Nature*, v. 335, p. 535-538.
- 1023 Furnes, H., de Wit, M., Staudigel, H., Rosing, M., and Muehlenbachs, K., 2007, A vestige of
1024 Earth's oldest ophiolite: *Science*, v. 215, p. 1704-1707.
- 1025 Griffin, W. L., McGregor, V. R., Nutman, A. P., Taylor, P. N., and Bridgwater, D., 1980,
1026 Early Archaean granulite-facies metamorphism south of Ameralik: *Earth and Planetary
1027 Science Letters*, v. 50, p. 59-74.
- 1028 Hamilton, P. J., O'Nions, R. K., Evensen, N. H., Bridgwater, D., and Allaart, J. H., 1978,
1029 Sm-Nd isotopic investigations of Isua supracrustals and implications for mantle
1030 evolution: *Nature*, v. 272, p. 41-43.
- 1031 Harris, N., 2007, Channel flow and the Himalayan–Tibetan orogen: a critical review: *Journal
1032 of the Geological Society, London*, v. 164, p. 511-523.
- 1033 Hiess, J., Bennett, V. C., Nutman, A. P., and Williams, I. S., 2009, In situ U–Pb, O and Hf
1034 isotopic compositions of zircon and olivine from Eoarchaeon rocks, West Greenland:
1035 New insights to making old crust: *Geochimica et Cosmochimica Acta*, v. 73 p.
1036 4489–4516.
- 1037 Hiess, J., Bennett, V. C., Nutman, A. P., and Williams, I. S., 2011, Archaean fluid-assisted
1038 crustal cannibalism recorded by low $\delta^{18}\text{O}$ and negative $\epsilon_{\text{Hf}}(\text{T})$ isotopic signatures of
1039 West Greenland granite zircon: *Contributions to Mineralogy and Petrology*, v. 161, p.
1040 1027-1050, DOI 10.1007/s00410-010-0578-z.
- 1041 Hoffmann, J. E., Münker, C., Polat, A., König, S., Mezger, K., and Rosing, M. T., 2010,
1042 Highly depleted Hadean mantle reservoirs in the sources of early Archean arc-like
1043 rocks, Isua supracrustal belt, southern West Greenland: *Geochimica et Cosmochimica
1044 Acta*, v. 74, p. 7236-7260.
- 1045 Hoffmann, J. E., Münker, C., Naeraa, T., Rosing, M. T., Garbe-Schönberg D., and
1046 Svahnberg, H., 2011a, Mechanisms of Archean crust production inferred from high
1047 precision HFS systematics in TTGs: *Geochimica et Cosmochimica Acta*, v. 75, p.
1048 4175-4178.
- 1049 Hoffmann, J. E., Münker, C., Polat, A., Rosing, M. T. and Schulz, T., 2011b, The origin of
1050 decoupled Hf-Nd isotope compositions in Eoarchean rocks from southern West
1051 Greenland: *Geochimica et Cosmochimica Acta*, v. 75, p. 6610-6628.
- 1052 Hollister, L. S., and Crawford, M. L., 1986, Melt-enhanced deformation: A major tectonic
1053 process: *Geology*, v. 14, p. 558-561.
- 1054 Horie, K., Nutman, A. P., Friend, C. R. L., and Hidaka, H., 2010, The complex age of
1055 orthogneiss protoliths exemplified by the Eoarchaeon Itsaq Gneiss Complex (Greenland):
1056 SHRIMP and old rocks: *Precambrian Research*, v. 181, p. 25-43.

- 1057 Iizuka, T., Komiya, T., Ueno, Y., Katayama, I., Uehara, Y., Maruyama, S., Hirata, T.,
1058 Johnson, S. P., and Dunkley, D. J., 2007, Geology and zircon geochronology of the
1059 Acasta Gneiss Complex, northwestern Canada: New constraints on its tectonothermal
1060 history: *Precambrian Research*, v. 153, p. 179–208.
- 1061 Jacobsen, S. B., and Dymek, R. F., 1987, Nd and Sr isotope systematics of clastic
1062 metasediments from Isua, West Greenland: Identification of pre-3.8 Ga differentiated
1063 crustal components: *Journal of Geophysical Research*, v. 93, p. 338-354.
- 1064 Jenner, F. E., Bennett, V. C., Nutman, A. P., Friend, C. R. L., Norman, M. D., and Yaxley, G.,
1065 2009, Evidence for subduction at 3.8 Ga: Geochemistry of arc-like metabasalts from the
1066 southern edge of the Isua Supracrustal Belt: *Chemical Geology*, v. 261, p. 82-99.
- 1067 Kamber, B.S., and Moorbath, M., 1998, Initial Pb of the Amîtsoq gneiss revisited:
1068 implication for the timing of early Archaean crustal evolution in West Greenland:
1069 *Chemical Geology*, v. 150, p. 19-41.
- 1070 Kamber, B. S., Collerson, K. D., Moorbath, S., Whitehouse, M. J., 2003, Inheritance of early
1071 Archean Pb-isotope variability from long-lived Hadean protocrust: *Contributions to
1072 Mineralogy and Petrology*, v. 145, p. 25-46
- 1073 Kamber, B. S., Whitehouse, M. J., Bolhar, R., and Moorbath, S., 2005, Volcanic resurfacing
1074 and the early terrestrial crust: Zircon U-Pb and REE constraints from the Isua
1075 Greenstone Belt, southern West Greenland: *Earth and Planetary Science Letters*, v.
1076 240, p. 276-290.
- 1077 Kemp, A. I. S., Foster, G. L., Scherstén, A., Whitehouse, M. J., Darling, J., and Storey, C.,
1078 2009, Concurrent Pb-Hf isotope analysis of zircon by laser ablation multi-collector
1079 ICP-MS, with implications for the crustal evolution of Greenland and the Himalayas:
1080 *Chemical Geology*, v. 261, p. 244-260.
- 1081 Kinny, P. D., 1986, 3820 Ma zircons from a tonalitic Amîtsoq gneiss in the Godthåb district
1082 of southern West Greenland: *Earth and Planetary Science Letters*, v. 79, p. 337-347.
- 1083 Kinny P. D., 1987, An ion-microprobe study of uranium-lead and hafnium isotopes in natural
1084 zircon: Ph.D. Thesis, Australian National University.
- 1085 Kinny, P. D., and Nutman, A. P., 1996, Zirconology of the Meeberrie gneiss, Yilgarn Craton,
1086 Western Australia: an early Archaean migmatite: *Precambrian Research*, v. 78, p.
1087 165-178.
- 1088 Klemperer, S. L., 2006, Crustal flow in Tibet: geophysical evidence for the physical state of
1089 Tibetan lithosphere, and inferred patterns of active flow: In: Law, R.D., Searle, M.P.
1090 and Godin, L. (eds) *Channel Flow, Ductile Extrusion and Exhumation in Continental
1091 Collision Zones*. Geological Society, London, Special Publications, v. 268, p. 39–70.
- 1092 Komiya, T., Maruyama, S., Masuda, T., Appel, P.W.U., and Nohda, S., 1999, The 3.8-3.7 Ga
1093 plate tectonics on the Earth; Field evidence from the Isua accretionary complex, West
1094 Greenland: *Journal of Geology*, v. 107, p. 515-554.

- 1095 Liu, D., Wan, Y., Wu, J. S., Wilde, S. A., Zhou, H. Y., Dong, C. Y., and Yin, X. Y., 2007,
1096 Eoarchean rocks and zircons in the North China Craton: van Kranendonk, M.J.,
1097 Smithies, R.H. and Bennett, V.C. (eds) *Earth's Oldest Rocks*. Elsevier, pp. 251-274.
- 1098 McGregor, V.R., 1968, Field evidence of very old Precambrian rocks in the Godthåb
1099 area, West Greenland: *Rapport Grønlands Geologiske Undersøgelse*, v. 15, p.
1100 31-35.
- 1101 McGregor, V.R., 1973, The early Precambrian gneisses of the Godthåb district, West
1102 Greenland: *Philosophical Transactions of the Royal Society of London*, v. A273, p.
1103 343-358.
- 1104 McCulloch, M. T., and Woodhead, J. D., 1993, Lead isotopic evidences for deep crustal-scale
1105 fluid transport during granite petrogenesis: *Geochimica et Cosmochimica Acta*, v. 57,
1106 p. 659-674.
- 1107 McGregor, V. R., 2000, Initial Pb of the Amîtsoq gneiss revisited: Implications for the timing
1108 of early Archaean crustal evolution in West Greenland—Comment: *Chemical
1109 Geology*, v.166, p. 301-308.
- 1110 McGregor, V. R., and Mason, B., 1977, Petrogenesis and geochemistry of metabasaltic and
1111 metasedimentary enclaves in the Amîtsoq gneisses, West Greenland: *American
1112 Mineralogist*, v. 62, p. 887-904.
- 1113 McGregor, V. R., Friend, C. R. L., and Nutman, A. P., 1991, The late Archaean mobile belt
1114 through Godthåbsfjord, southern West Greenland: a continent-continent collision
1115 zone?: *Bulletin of the Geological Society of Denmark*, v. 39, p. 179-197.
- 1116 Moorbath, S., 1975, Evolution of Precambrian crust from strontium isotopic evidence:
1117 *Nature*, v. 254, p. 395-398.
- 1118 Moorbath, S., 1994, Age of the oldest rocks with biological components: *Journal of
1119 Biological Physics*, v. 20, p. 85-94.
- 1120 Moorbath, S., 2005: Oldest rocks, earliest life, heaviest impacts, and the Hadean–Archaean
1121 transition: *Applied Geochemistry*, v. 20, p. 819–824.
- 1122 Moorbath, S., O’Nions, R. K., and Pankhurst, R. J., 1973, Early Archaean age for the Isua
1123 iron formation, West Greenland: *Nature*, v. 245, p. 138-139.
- 1124 Moorbath, S., O’Nions, R. K., Pankhurst, R. J., Gale, N. H., and McGregor, V. R., 1972,
1125 Further rubidium-strontium age determinations on the very early Precambrian rocks of
1126 the Godthåb district, West Greenland: *Nature*, v. 240, p. 78-82.
- 1127 Moorbath, S., Allaart, J. H., Bridgwater, D., and McGregor, V. R., 1977, Rb-Sr ages of early
1128 Archaean supracrustal rocks and Amîtsoq gneisses at Isua: *Nature*, v. 270, p. 43-45.
- 1129 Myers, J.S., 2001, Protoliths of the 3.8–3.7 Ga Isua greenstone belt, West Greenland:
1130 *Precambrian Research*, v. 105, p. 129-141.
- 1131 Nagel, T. J., Hoffmann, J. E., Münker, K., 2012, Generation of Eoarchean
1132 tonalite-trondhjemite-granodiorite series from thickened mafic arc crust: *Geology*, v.
1133 40, p. 375-378; doi:10.1130/G32729.1

- 1134 Nutman, A. P., 1984, Early Archaean crustal evolution of the Isukasia area, southern West
1135 Greenland: In: Kröner, A. & Greiling, R. (eds) Precambrian Tectonics Illustrated,
1136 Stuttgart, E. Schweitzerbart'sche Verlagsbuchhandlung.
- 1137 Nutman, A. P., 2006, Antiquity of the Oceans and Continents: Elements, v. 2, p. 223-227.
- 1138 Nutman, A. P., and Bridgwater, D., 1986, Early Archaean Amîtsoq tonalites and granites
1139 from the Isukasia area, southern West Greenland: Development of the oldest-known
1140 sial: Contributions to Mineralogy and Petrology, v. 94, p. 137-148.
- 1141 Nutman, A. P., and Friend, C. R. L., 2007a, Terranes with ca. 2715 and 2650 Ma
1142 high-pressure metamorphisms juxtaposed in the Nuuk region, southern West
1143 Greenland: Complexities of Neoproterozoic collisional orogeny: Precambrian Research,
1144 v. 155, p. 159-203.
- 1145 Nutman, A. P., and Friend, C. R. L., 2009, New 1:20000 geological maps, synthesis and
1146 history of the Isua supracrustal belt and adjacent gneisses, Nuuk region, southern West
1147 Greenland: A glimpse of Eoarchaean crust formation and orogeny: Precambrian
1148 Research, v. 172, p. 189-211.
- 1149 Nutman, A. P., Friend, C. R. L., and Bennett, V., 2004a, Dating of the Ameralik dyke
1150 swarms of the Nuuk district, southern West Greenland: Mafic intrusion events
1151 starting from c. 3510 Ma: Journal of the Geological Society, London, v. 161, p.
1152 421-430.
- 1153 Nutman, A. P., Friend, C. R. L., and Paxton, S., 2009, Detrital zircon sedimentary
1154 provenance ages for the Eoarchaean Isua supracrustal belt southern West
1155 Greenland: Juxtaposition of ca. 3700 Ma juvenile arc assemblages against an
1156 older complex with 3920-3800 Ma components: Precambrian Research, v. 172,
1157 p. 212-233.
- 1158 Nutman, A. P., Bridgwater, D., and Fryer, B., 1984b, The iron rich suite from the Amîtsoq
1159 gneisses of southern West Greenland: Early Archaean plutonic rocks of mixed crustal
1160 and mantle origin: Contributions to Mineralogy and Petrology, v. 87, p. 24-34.
- 1161 Nutman, A. P., Friend, C. R. L., Baadsgaard, H., and McGregor, V. R., 1989,
1162 Evolution and assembly of Archaean gneiss terranes in the Godthåbsfjord
1163 region, southern West Greenland: structural, metamorphic and isotopic
1164 evidence: Tectonics, v. 8, p. 573-589.
- 1165 Nutman, A. P., Friend, C. R. L., Kinny, P. D., and McGregor, V. R., 1993, Anatomy of an
1166 Early Archaean gneiss complex: 3900 to 3600 Ma crustal evolution in southern West
1167 Greenland: Geology, v. 21, p. 415-418.
- 1168 Nutman, A. P., Allaart, J. H., Bridgwater, D., Dimroth, E., and Rosing, M. T., 1984a,
1169 Stratigraphic and geochemical evidence for the depositional environment of the early
1170 Archaean Isua supracrustal belt, southern West Greenland: Precambrian Research, v.
1171 25, p. 365-396.

- 1172 Nutman, A. P., Kinny, P. D., Compston, W., and Williams, I. S., 1991, SHRIMP U-Pb zircon
1173 geochronology of the Narryer Gneiss Complex, Western Australia: *Precambrian*
1174 *Research*, v. 52, p. 275-300.
- 1175 Nutman, A. P., McGregor, V. R., Friend, C. R. L., Bennett, V. C., and Kinny, P. D., 1996,
1176 The Itsaq Gneiss Complex of southern West Greenland; the world's most extensive
1177 record of early crustal evolution (3900-3600 Ma): *Precambrian Research*, v. 78, p.
1178 1-39.
- 1179 Nutman, A. P., Bennett, V. C., Friend, C. R. L., and Rosing, M. T., 1997a, ~3710 and
1180 3790 Ma volcanic sequences in the Isua (Greenland) supracrustal belt; structural
1181 and Nd isotope implications: *Chemical Geology*, v. 141, p. 271-287.
- 1182 Nutman, A. P., Mozjzsis, S., and Friend, C. R. L., 1997b, Recognition of ≥ 3850 Ma water-lain
1183 sediments in West Greenland and their significance for the early Archaean Earth:
1184 *Geochimica et Cosmochimica Acta*, v. 61, p. 2475-2484.
- 1185 Nutman, A. P., Bennett, V. C., Friend, C. R. L., and Norman, M., 1999, Meta-igneous
1186 (non-gneissic) tonalites and quartz-diorites from an extensive ca. 3800 Ma terrain south
1187 of the Isua supracrustal belt, southern West Greenland: constraints on early crust
1188 formation: *Contributions to Mineralogy and Petrology*, v. 137, p. 364-388.
- 1189 Nutman, A. P., Friend, C. R. L., Bennett, V. C., and McGregor, V. R., 2000, The early
1190 Archaean Itsaq Gneiss Complex of southern West Greenland: The importance of field
1191 observations in interpreting dates and isotopic data constraining early terrestrial
1192 evolution: *Geochimica et Cosmochimica Acta*, v. 64, p. 3035-3060.
- 1193 Nutman, A. P., McGregor, V. R., Shiraishi, K., Friend, C. R. L., Bennett, V. C., and Kinny, P.
1194 D., 2002a, ≥ 3850 Ma BIF and mafic inclusions in the early Archaean Itsaq Gneiss
1195 Complex around Akilia, southern West Greenland? The difficulties of precise dating of
1196 zircon-free protoliths in migmatites: *Precambrian Research*, v. 117, p. 185-224.
- 1197 Nutman, A. P., Friend, C. R. L., and Bennett, V. C., 2002b, Evidence for 3650-3600 Ma
1198 assembly of the northern end of the Itsaq Gneiss Complex, Greenland: Implication for
1199 early Archean tectonics: *Tectonics*, v. 21, article 5
- 1200 Nutman, A. P., Friend, C. R. L., Barker, S. S., and McGregor, V. R., 2004b, Inventory and
1201 assessment of Palaeoarchaeoan gneiss terrains and detrital zircons in southern West
1202 Greenland: *Precambrian Research*, v. 135, p. 281-314.
- 1203 Nutman, A. P., Friend, C. R. L., Horie, H., and Hidaka, H., 2007a, Construction of pre-3600
1204 Ma crust at convergent plate boundaries, exemplified by the Itsaq Gneiss Complex of
1205 southern West Greenland: In: van Kranendonk, M.J., Smithies, R.H., & Bennett, V.C.
1206 (eds) *Earth's Oldest Rocks*. Elsevier, pp. 187-218.
- 1207 Nutman, A. P., Bennett, V. C., Friend, C. R. L., Horie, K., and Hidaka, H., 2007b, ~3850 Ma
1208 tonalites in the Nuuk region, Greenland: Geochemistry and their reworking within an
1209 Eoarchaeoan gneiss complex: *Contributions to Mineralogy and Petrology*, v. 154, p.
1210 385-408.

- 1211 Nutman, A. P., Friend, C. R. L., Bennett, V. C., Wright, D., and Norman, M. D., 2010, ≥ 3700
1212 Ma pre-metamorphic dolomite formed by microbial mediation in the Isua supracrustal
1213 belt (W. Greenland): Simple evidence for early life?: *Precambrian Research*, v. 183, p.
1214 725–737
- 1215 Nutman, A. P., Bennett, V. C., and Friend, C. R. L., 2011, Waves and weathering at 3.7 Ga:
1216 Geologic evidence for an equitable climate under the faint early Sun: *Australian*
1217 *Journal of Earth Sciences*, DOI:10.1080/08120099.2012.618512
- 1218 Nutman, A. P., Bennett, V. C., and Friend, C. R. L., in press, The emergence of the
1219 Eoarchean proto-arc: evolution of a c. 3700 Ma convergent plate boundary at Isua,
1220 southern West Greenland: *Special Publications of the Geological Society, London*,
1221 revised version accepted February 2013.
- 1222 Næraa, T., Schersten, A., Rosing, M. T., Kemp, A. I. S., Hoffmann, J. E., Kokfelt, T. F., and
1223 Whitehouse, M. J., 2012, Hafnium isotope evidence for the transition in the dynamics
1224 of continental growth 3.2 Gyr ago: *Nature*, v. 485, p. 627-630.
- 1225 O’Neil, J., Maurice, C., Stevenson, R. K., Larocque, J., Cloquet, C., David, J., and Francis,
1226 D., 2007, The geology of the 3.8 Ga Nuvvuagittuq (Porpoise Cove) greenstone belt,
1227 northeastern Superior Province, Canada: In: van Kranendonk, M.J., Smithies, R.H., &
1228 Bennett, V.C. (eds) *Earth’s Oldest Rocks*. Elsevier, pp. 219-250.
- 1229 Polat, A., and Hofmann, A. W., 2003, Alteration and geochemical patterns in the 3.7-3.8 Ga
1230 Isua greenstone belt, West Greenland: *Precambrian Research*, v. 126, p. 197-218.
- 1231 Polat, A., Hofmann, A. W., and Rosing, M. T., 2002, Boninite-like volcanic rocks in the
1232 3.7-3.8 Ga Isua greenstone belt, West Greenland: geochemical evidence for
1233 intra-oceanic subduction processes in the early Earth: *Chemical Geology*, v. 184, p.
1234 231-254.
- 1235 Pope, E. C., Bird, D. K., Rosing, M. T., 2012, Isotope composition and volume of Earth’s
1236 early oceans: *Proceedings of the National Academy of Sciences of the United States of*
1237 *America*, doi: 10.1073/pnas.1115705109
- 1238 Ren, J., Tamaki, K., Li, S. and Zhang, J., 2002, Late Mesozoic and Cenozoic rifting and its
1239 dynamic setting in Eastern China and adjacent areas: *Tectonophysics*, v. 344, p.
1240 175-205.
- 1241 Rey, P., and Coltice, N., 2008, A Neoproterozoic lithospheric strengthening and the coupling of
1242 Earth’s geochemical reservoirs: *Geology*, v. 36, p. 635-638.
- 1243 Rizo, H., Boyet, M., Blichert-Toft, J., and Rosing, M. T., 2011, Combined Nd and Hf isotope
1244 evidence for deep-seated source of Isua lavas: *Earth and Planetary Science Letters*, v.
1245 312, p. 267-279.
- 1246 Rosing, M.T., 1999, ^{13}C -depleted carbon microparticles in >3700 Ma sea-floor sedimentary
1247 rocks from West Greenland: *Science*, v. 283, p. 674-676.

- 1248 Rosing, M. T., Rose, N. M., Bridgwater, D., and Thomsen, H. S., 1996, Earliest part of the
1249 Earth's stratigraphic record: A reappraisal of the >3.7 Ga Isua (Greenland) supracrustal
1250 sequence: *Geology*, v. 24, p. 43-46.
- 1251 Sandiford, M., 1989, Horizontal structures in granulite terrains: A record of mountain
1252 building or mountain collapse?: *Geology*, v. 17, p. 449-452.
- 1253 Shervais, J. W., 2001, Birth, death, and resurrection: The life cycle of suprasubduction zone
1254 ophiolites: *Geochemistry Geophysics Geosystems*, paper number 2000GC000080.
- 1255 Schiøtte, L., Compston, W., and Bridgwater, D., 1989a, Ion probe U-Th-Pb zircon dating of
1256 polymetamorphic orthogneisses from northern Labrador, Canada: *Canadian Journal of*
1257 *Earth Sciences*, v. 26, p. 1533-1556.
- 1258 Schiøtte L., Compston W., and Bridgwater D., 1989b, U-Pb single zircon age for the Tinissaq
1259 gneiss of southern West Greenland: A controversy resolved: *Chemical Geology*, v. 79,
1260 p. 21-30.
- 1261 Solvang, M., 1999, An investigation of metavolcanic rocks from the eastern part of the Isua
1262 greenstone belt, Western Greenland: Geological Survey of Denmark and Greenland
1263 (GEUS) Internal Report, Copenhagen, Denmark, 62 pages.
- 1264 Steenfelt, A., Garde, A. A., and Moyen, J.-F., 2005, Mantle wedge involvement in the
1265 petrogenesis of Archaean grey gneisses in West Greenland: *Lithos*, v. 79, p. 207-228.
- 1266 Vervoort, J. D., and Blichert-Toft, J., 1999, Evolution of the depleted mantle: Hf evidence
1267 from juvenile rocks through time: *Geochimica et Cosmochimica Acta*, v. 63, p.
1268 533-556.
- 1269 Wei, W., Xu, J. D., Zhao, D. P., and Shi, Y. L., 2012, East Asia mantle tomography: New
1270 insight into plate subduction and intraplate volcanism: *Journal of Asian Earth Sciences*,
1271 v. 60, p. 88-103.
- 1272 White, R. V., Crowley, J. L., and Myers, J. S., 2000, Earth's oldest well-preserved
1273 mafic dyke swarms in the vicinity of the Isua greenstone belt, southern West
1274 Greenland: *Geology of Greenland Survey Bulletin*, v. 186, p. 65-72.
- 1275 Whitehouse, M. J., Kamber, B. S., and Moorbath, S., 1999, Age significance of U-Th-Pb
1276 zircon data from early Archaean rocks of west Greenland – a reassessment based on
1277 combined ion-microprobe and imaging studies: *Chemical Geology*, v. 160, p. 201-224.
- 1278 Willbold, M., Elliott, T., and Moorbath, S., 2001, The tungsten isotopic composition of the
1279 Earth's mantle before the terminal bombardment: *Nature*, v. 477, p. 195-198, doi:
1280 10.1038/nature10399.
- 1281 Yang, J. H., Wu, F. Y., Chung, S. L., Lo, C. H., Wilde, S. A., and Davis, G. A., 2007, Rapid
1282 exhumation of the Liaonan metamorphic core complex: Inferences from $^{40}\text{Ar}/^{39}\text{Ar}$
1283 thermochronology and implications for Late Mesozoic extension in the eastern North
1284 China Craton: *Bulletin of the Geological Society of America*, v. 119, p.1405-1414.
- 1285

1286

1287 **Figure captions**

1288 Figure 1. Geological map of the Nuuk region, displaying the Eoarchean Itsaq Gneiss Complex,
1289 summary of SHRIMP U/Pb zircon results on TTG rocks, showing the location of the oldest
1290 (≥ 3850 Ma) and youngest (3660 Ma) components. Localities mentioned in the text are
1291 indicated.

1292

1293 Figure 2. Timeline for the evolution of the Itsaq Gneiss Complex from 3900 to 3600 Ma. This
1294 is based on U-Pb zircon dating of more than 160 rocks integrated with geological mapping.

1295

1296 Figure 3. Schematic cross-sections illustrating state of the Itsaq Gneiss Complex at the end of
1297 the Isukasian orogeny. (A) Shows a rare area on the hills north of Amiitsoq (Fig. 1) where
1298 (meta) detrital sedimentary rocks deposited at 3620-3600 Ma are invaginated with ~3660 Ma
1299 tonalitic basement, and then folded and metamorphosed together at ~3580-3560 Ma (Friend
1300 and Nutman, 2005a). This is a rare sample of the upper crust during the Isukasian orogeny. (B)
1301 Reconstructs the Isua area, with a schematic cross section through the Isua supracrustal belt.
1302 Note the juxtaposition of rocks with different 3650-3600 Ma metamorphic grade across
1303 extensional structures. (C) Is a schematic representation of the lower crust. 3900-3660 Ma
1304 juvenile crustal rocks are soaked in 3660-3600 Ma neosome. Prevalent metamorphism is upper
1305 amphibolite to low-pressure granulite facies. 3640 Ma gabbro-granite composite intrusions
1306 show evidence of synmagmatic extension. (D) is a fusion of A, B and C, to reconstruct the
1307 crustal architecture late in the Isukasian orogeny.

1308

1309 Figure 4. Orthogneisses of the Itsaq Gneiss Complex. (A) Orthogneiss from the southern part of
1310 the Itsaq Gneiss Complex (63°50.920'N 51°39.894'W) that escaped strong superimposed
1311 Neoproterozoic deformation common in this part of the Complex. Note the variably deformed
1312 degree of the neosome (n) across this single outcrop. Knife for scale is 7 cm long. The tonalitic
1313 palaeosome (p) is variably modified by *in situ* anatexis and disruption by intruded granite and
1314 pegmatite veins. The pegmatites with hornblende \pm biotite pseudomorphs replacing original

1315 pyroxene are the products of Eoarchean dehydration melting under granulite facies conditions.
1316 ~3500 Ma Ameralik dykes traversing these outcrops (not shown in the frame of view) are
1317 weakly deformed and strongly discordant to the migmatite layering. However, they have been
1318 converted into amphibolite during superimposed Neoproterozoic upper amphibolite facies
1319 metamorphism. (B) Low strain zone in the ~3700 Ma tonalite domain north of the Isua
1320 supracrustal belt (65°10.749'N 50°01.020'W). Host ~3700 Ma meta-tonalites (t) are variably
1321 deformed, but locally preserve a weakly porphyritic texture, given by (recrystallized)
1322 plagioclase phenocrysts. Note these tonalites are devoid of *in situ* partial melt domains. They
1323 are traversed by a dioritic Inaluk dyke (In) and granite sheets (g). These outcrops are cut by
1324 completely non-deformed ~3500 Ma Ameralik dykes (not shown in the view), which contain
1325 relict igneous pyroxenes and plagioclase partially replaced by Neoproterozoic epidote amphibolite
1326 facies assemblages. (C) Early granite (g) in the ~3700 Ma terrane north of the Isua supracrustal
1327 belt (65°10.620'N 50°00.824'W). Note that these involve at least some *in situ* anatexis of the
1328 host tonalites (t), and the development of synplutonic ductile sigmoidal structures. Pen for scale
1329 is 15 cm long. (D) Homogeneous ~3810 Ma tonalite south of the Isua supracrustal belt
1330 (65°00.63'N 50°15.04'W; sample G97/18). Metatonalite is cut by an amphibolitized but not
1331 deformed ~3500 Ma Ameralik dyke (ad). This demonstrates that since the Eoarchean at this
1332 locality, there has been no deformation, but superimposed 'static' epidote amphibolite facies
1333 metamorphism. Preserved in the tonalites is a relict plagioclase-phyric texture. (E)
1334 Photomicrograph of G97/18 from the locality shown in (D) demonstrates the early alteration of
1335 plagioclase (plag-rx), followed by later static recrystallisation giving randomly orientated
1336 laths of biotite (bio) and epidote. Field of view is 2 mm wide. (F) Pre- ~3500 Ma strong
1337 cataclastic deformation affecting ~3700 Ma tonalites already intruded by Eoarchean granite
1338 sheets (65°09.253'N 50°03.150'W). The cataclastic textures were recrystallized in
1339 superimposed post Ameralik dyke epidote amphibolite facies metamorphism. Pen for scale is
1340 15 cm long. (G) Cataclastic gneiss showing alteration of plagioclase to albite + epidote + quartz
1341 (plag-rx) and the formation of ribbon quartz (qtz). Note the post kinematic growth of biotite
1342 across the fabric (bio). Field of view is 3 mm wide. (H) 3640 Ma augen granite gneisses with
1343 coeval mafic intrusions on the south coast of the mouth of Ameralik (64°10.900'N

1344 51°36.395'W). Augen granite (aug) is intruded by variably attenuated ferrogabbro dikes
1345 (notebook for scale). The dike in the middle view (d1) is only mildly attenuated, whereas those
1346 in the background (e.g. d2) are disrupted and becoming enclosed and incorporated within the
1347 augen granite. A5 notebook for scale.

1348

1349 Figure 5. Map the northern part of the Itsaq Gneiss Complex, covering the Isua supracrustal
1350 belt. This is based on revised mapping by Nutman & Friend (2009). Representative zircon age
1351 determinations without sample number indicated are by Nutman and co-workers (published).
1352 The dating locality with sample number G11/24 is presented in this paper. Line 'N' is an
1353 approximate boundary between a northern area where post- Ameralik dyke (<3500 Ma) ductile
1354 deformation is weak, from the south where it is strong. However, to the north there are still
1355 some zones of strong late ductile deformation, whereas to the south there are some areas that
1356 escaped this later deformation.

1357

1358 Figure 6. Summary diagram of initial ϵ_{Hf} values derived from mafic whole rocks and from
1359 felsic rocks based on pooled data from their crystallization age zircon populations. For the
1360 zircon data from Hiess and others (2009, 2011) and Naerra and others (2012), their published
1361 weighted mean values were used. For the Kemp and others (2009) and Amelin and others
1362 (2011) data, weighted means were calculated from domains whose $^{207}\text{Pb}/^{206}\text{Pb}$ age complied
1363 with the previously determined protolith age.. Mafic whole rock data are from Hoffmann and
1364 others (2010, 2011b) and a mafic isochron initial composition from Rizo and others (2011).

1365

1366 Figure 7. (A) Garnet + clinopyroxene + hornblende + plagioclase + quartz segregations within
1367 banded amphibolites (GPS 65°09.087'N 50°03.619'W), probably formed by dehydration
1368 partial melting. (B) CL images of representative zircons from segregation sample G11/24.
1369 Scale bar in all frames is 10 μm . Analytical errors on the $^{207}\text{Pb}/^{206}\text{Pb}$ ages are given at the 1 σ
1370 level. (C) $^{238}\text{U}/^{206}\text{Pb}$ – $^{207}\text{Pb}/^{206}\text{Pb}$ concordia diagram summarising SHRIMP U-Pb zircon dating
1371 from partial melt segregation G11/24. Analytical errors are depicted at the 2 σ level, and the

1372 results are presented in Appendix 1. A few strongly discordant analyses are outside of the range
1373 of this plot.

1374

1375 Figure 8. Summary of SHRIMP U-Pb zircon ages from the Itsaq gneiss complex. The data are
1376 presented as follows: (A) tonalitic rocks and acid-intermediate volcanic rocks from areas with
1377 minimal superimposed migmatization, mostly upper- middle-crustal levels in the northern part
1378 of the complex; (B) tonalitic rocks throughout the rest of the complex where there is evidence
1379 of pervasive high temperature migmatization; (C) granite intrusions in least migmatized upper-
1380 middle-crustal levels; (D) synkinematic granite intrusions along shear zones in upper-
1381 middle-crustal levels (E) granite and coeval gabbro intrusions in strongly migmatized
1382 lower-crustal levels. Inher = inherited (pre-magmatic) zircon cores. Met = <3600 Ma
1383 metamorphic zircon.

1384

1385

1386 **Appendix 1**

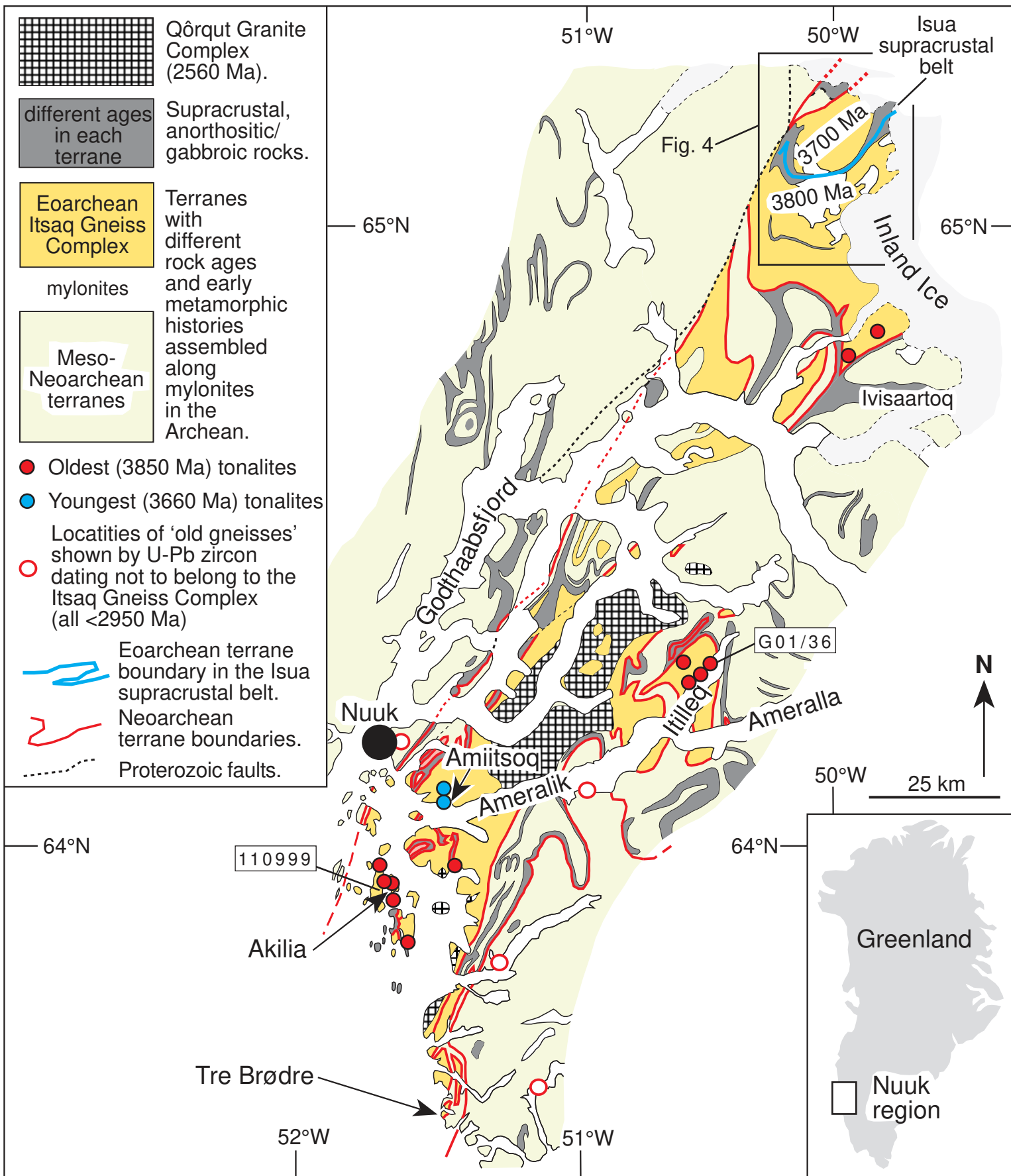
1387

1388

1389

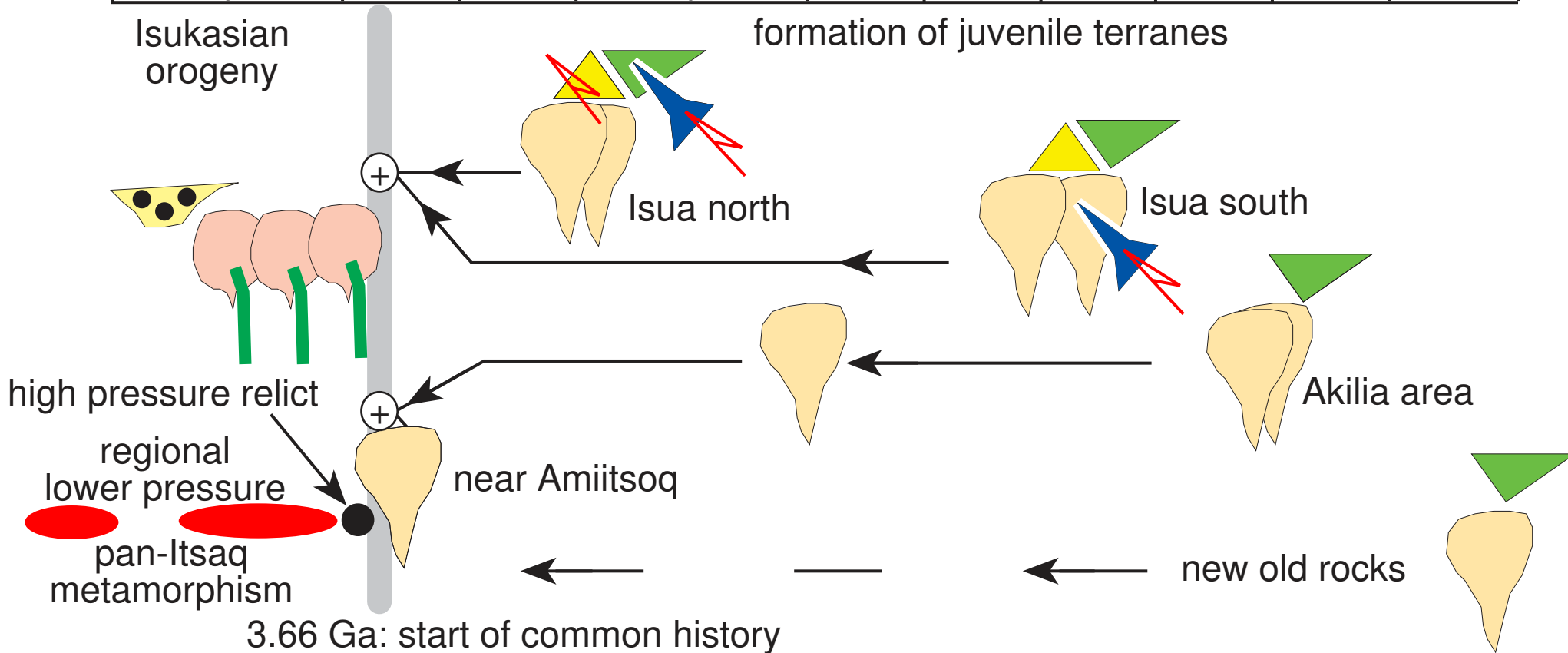
1390 **Appendix 1 Table caption**

1391 Appendix Table 1. Summary of SHRIMP U-Pb zircon data for high-pressure granulite
1392 segregation G11/24.



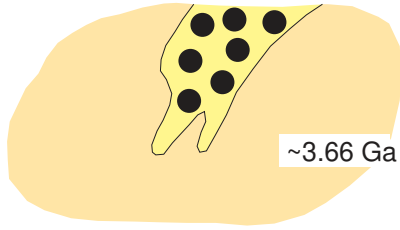
Itsaq Gneiss Complex time line: 3.9-3.6 Ga

3.60 Ga 3.70 3.80 3.90 Ga

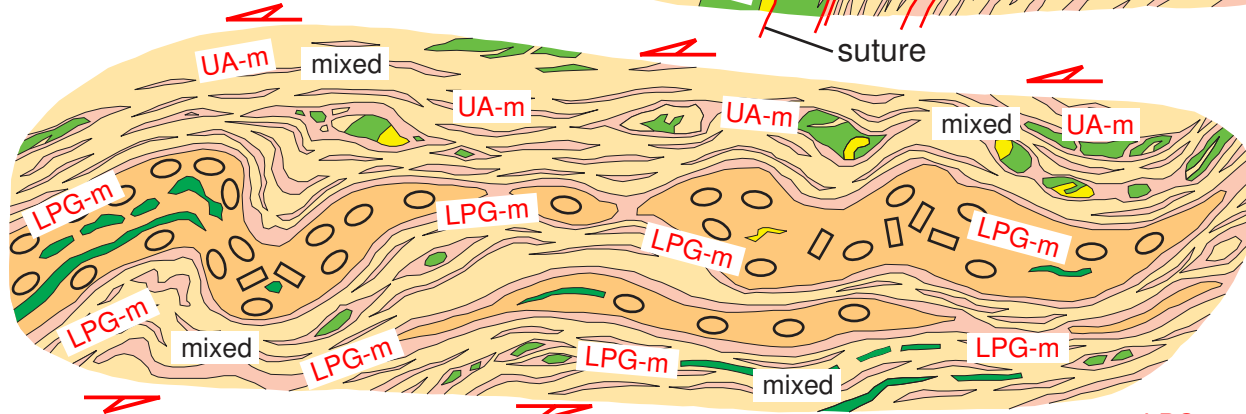
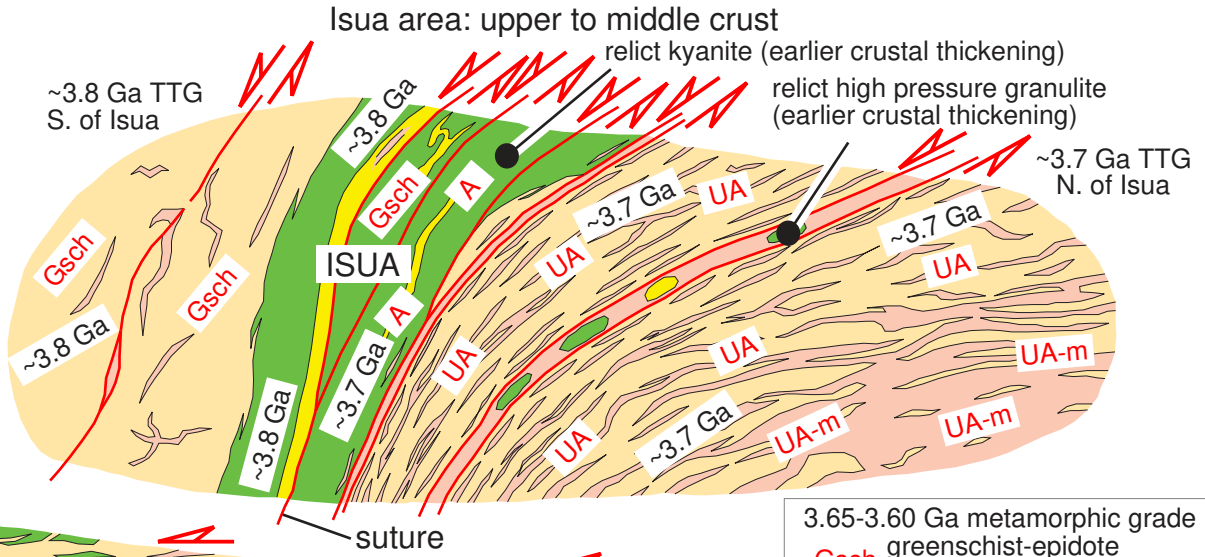


post assembly events	terrane assembly lineage	juvenile proto-arc development
detrital sedimentary basin(s)	terrane assembly lineage	juvenile TTG
ferrogabbros and crustally-derived granites	felsic volcanic rocks	intra-arc tectonic intercalation
		mafic volcanic rocks & gabbros
		mantle dunites

hills N. of Amitsoq; upper crust



Tectonic interpretation of the Itsaq Gneiss Complex (shown following 3.57 Ga folding)

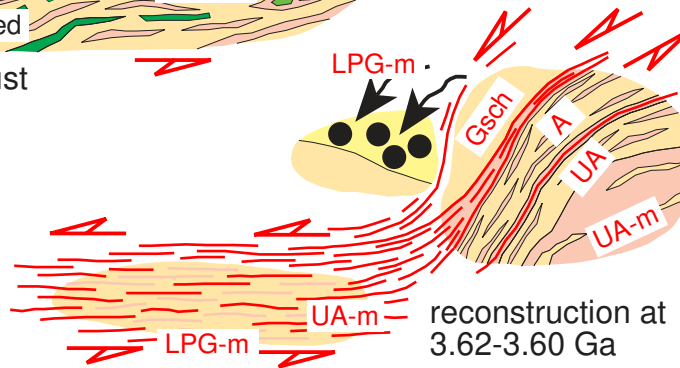


most of southern Itsaq Gneiss Complex; lower crust

3.65-3.60 Ga metamorphic grade

- Gsch greenschist-epidote amphibolite facies
- A amphibolite facies
- UA upper amphibolite facies
- UA-m amphibolite facies migmatites
- LPG-m low pressure granulite facies migmatites

	3.62-3.60 Ga detrital sedimentary rocks
	3.64 Ga ferrogabbro and ferrodiorite
	3.64 Ga augen gneisses
	3.65-3.62 Ga crustally-derived granite
	juvenile TTG rocks
	chemical sedimentary rocks
	mafic-intermediate supracrustal rocks

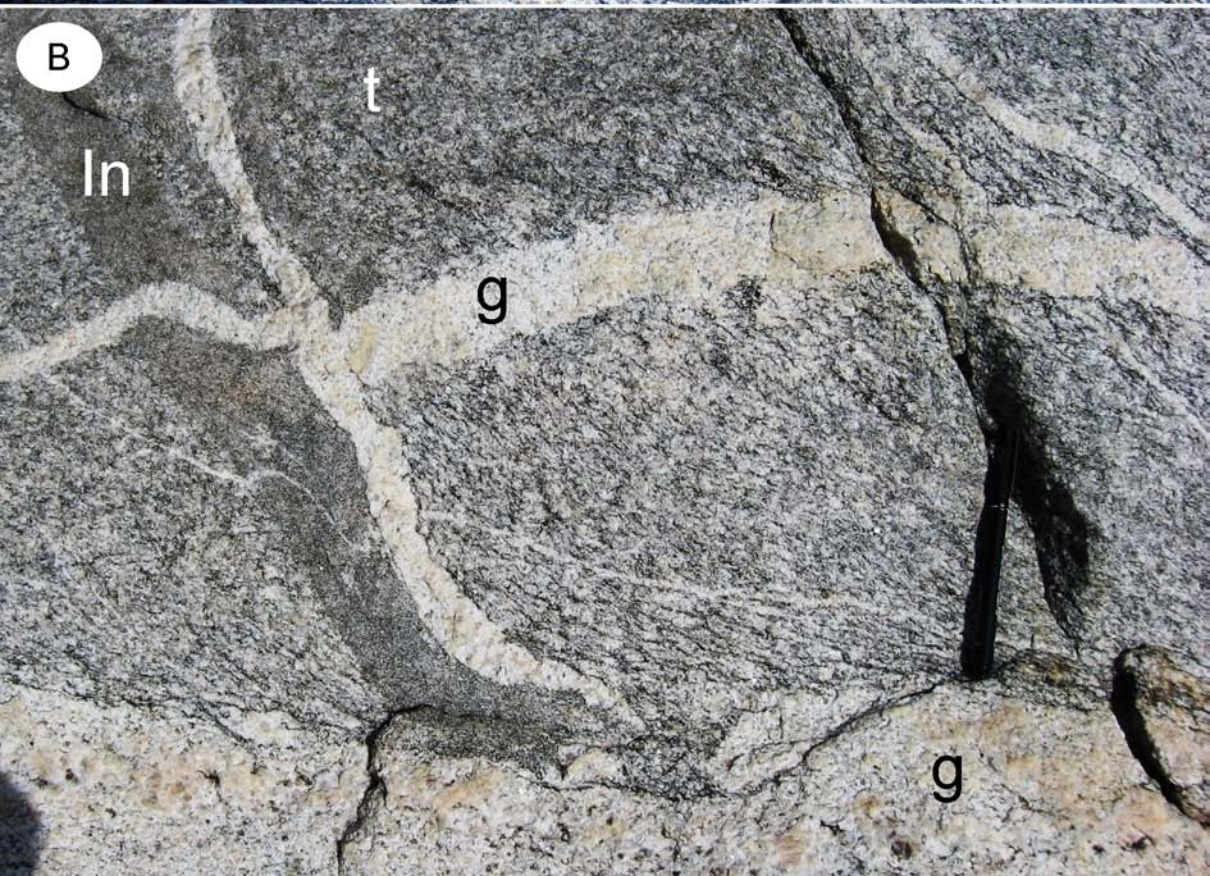
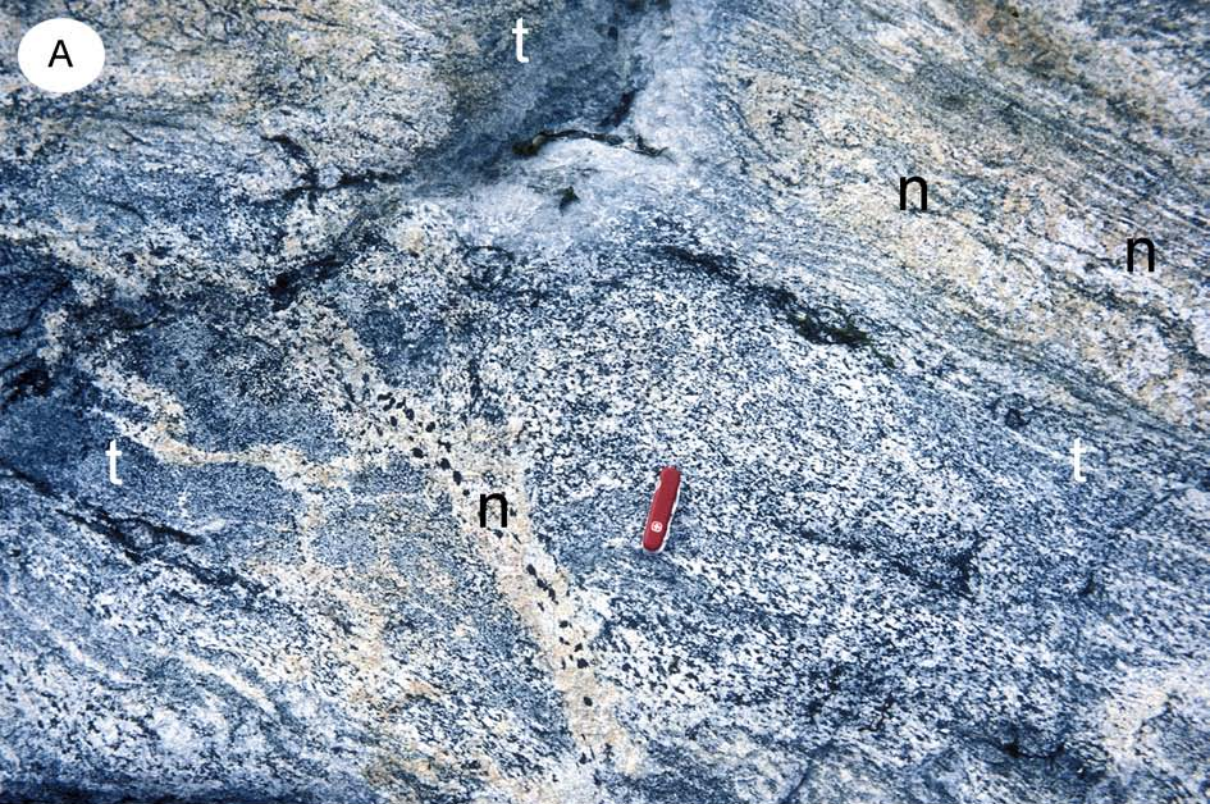


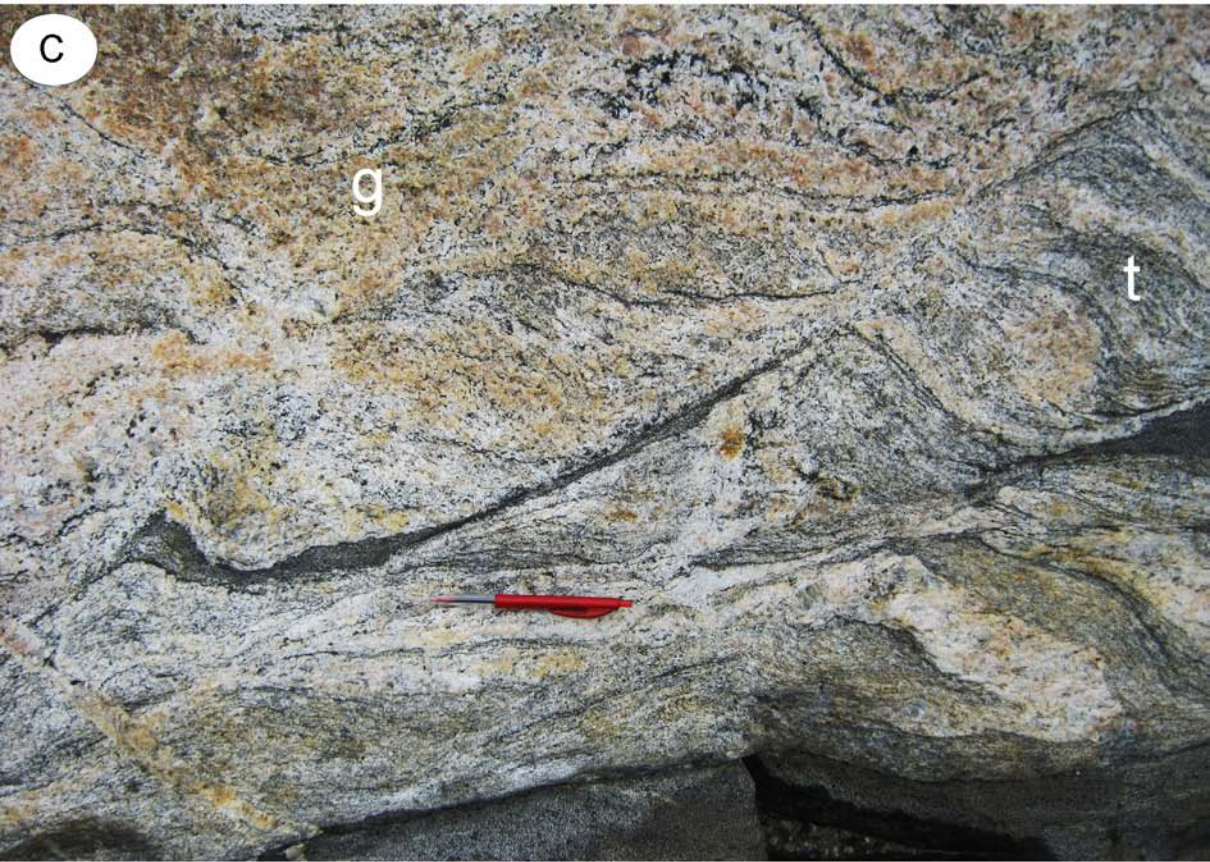
reconstruction at 3.62-3.60 Ga

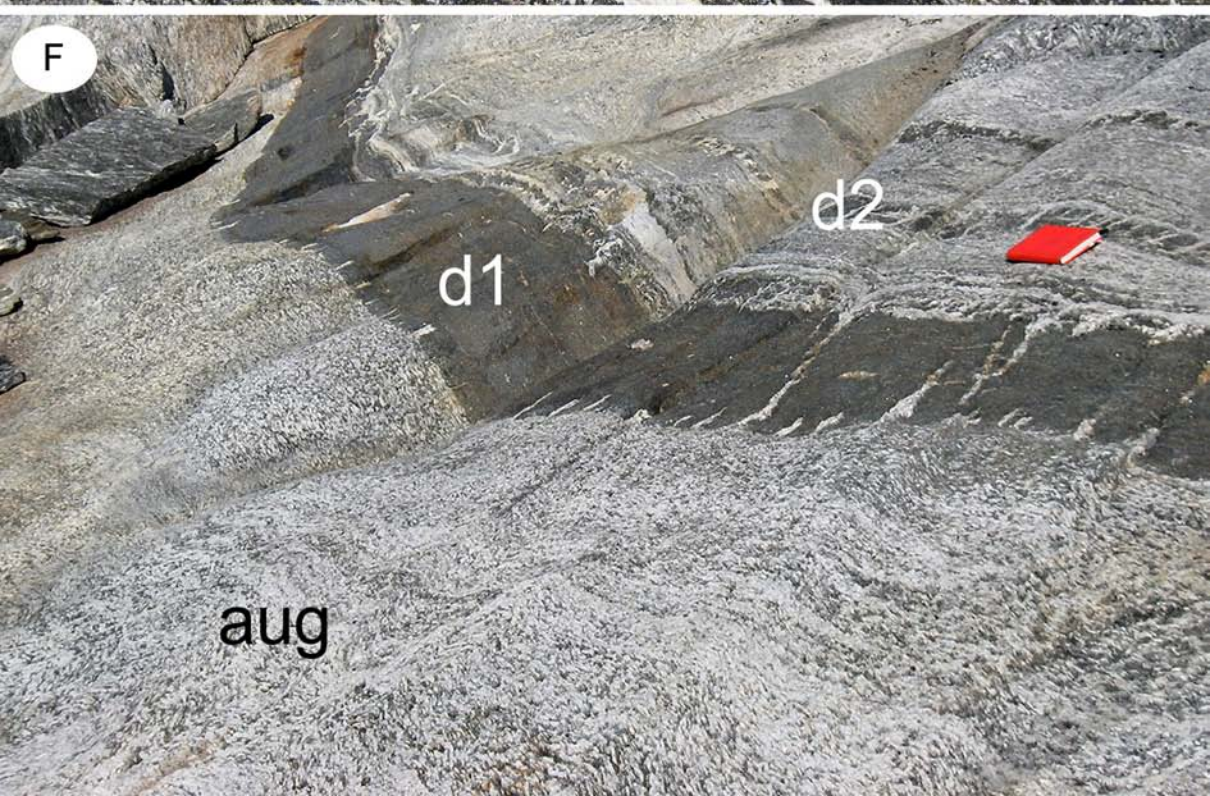
Ages of juvenile crustal components

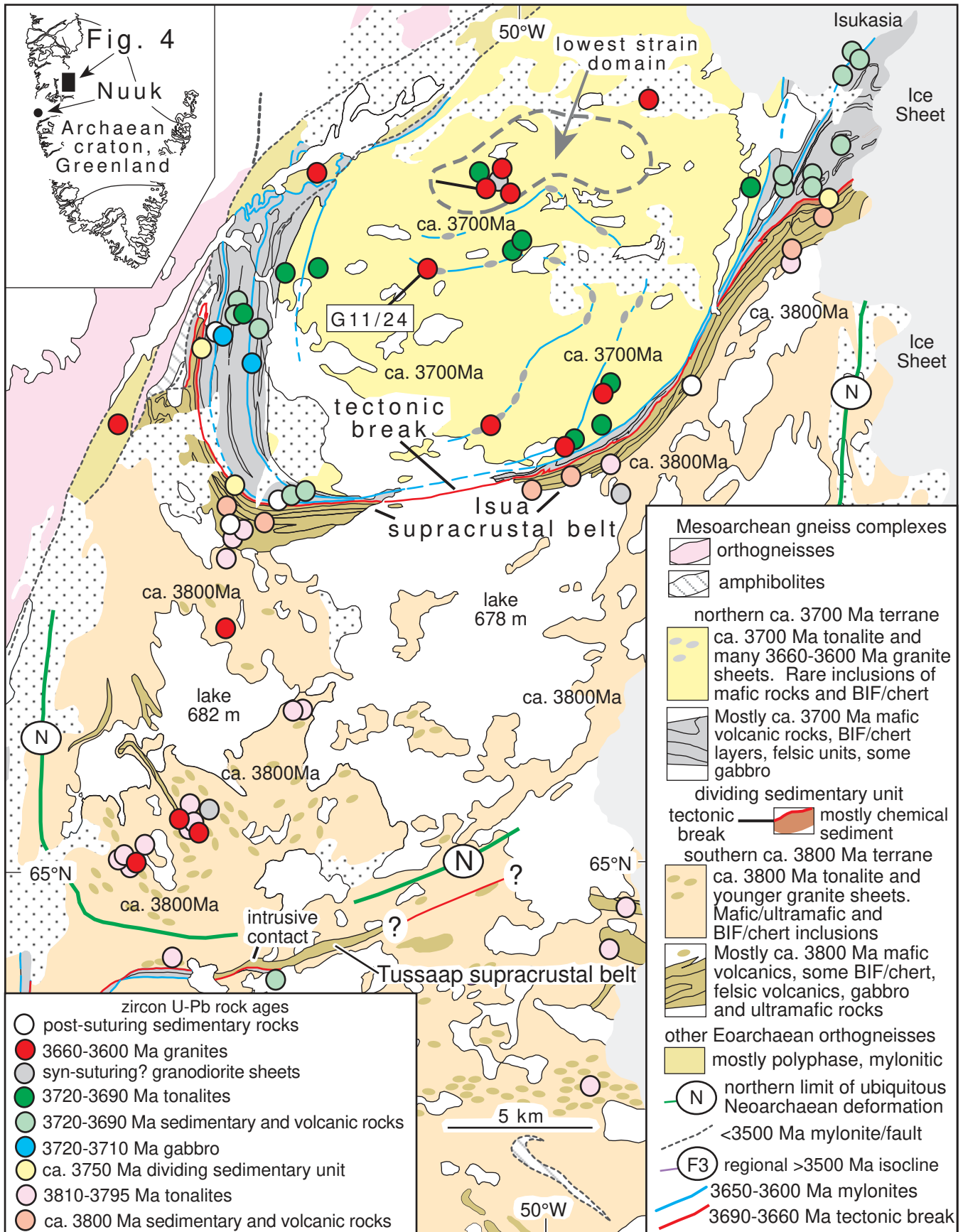
~3.66 Ga; rare, found in Amitsoq area ~3.7 Ga & ~3.8 Ga; juxtaposed in Isua area

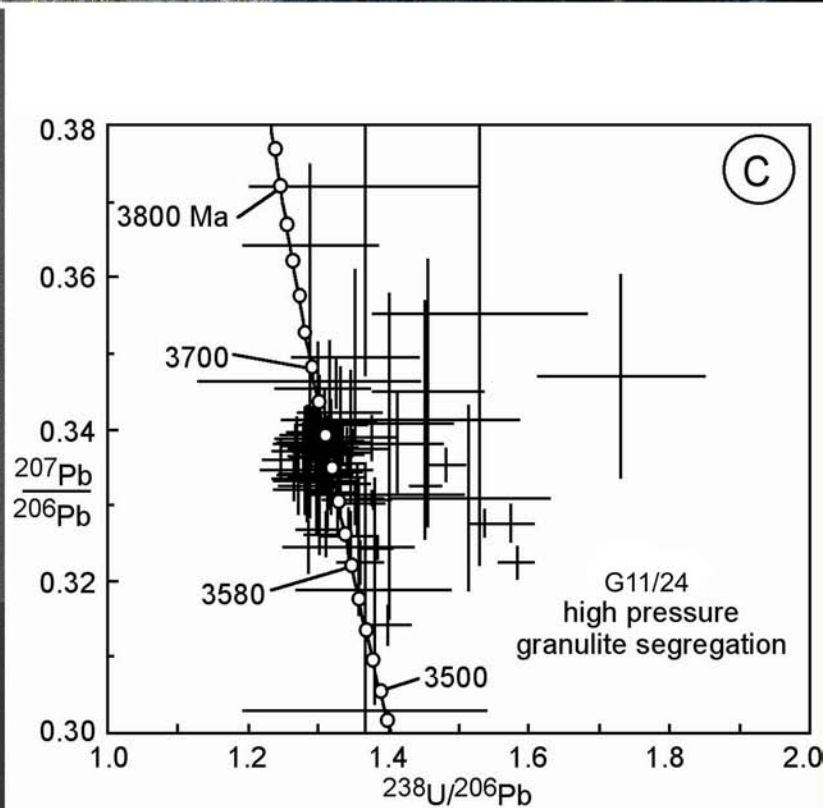
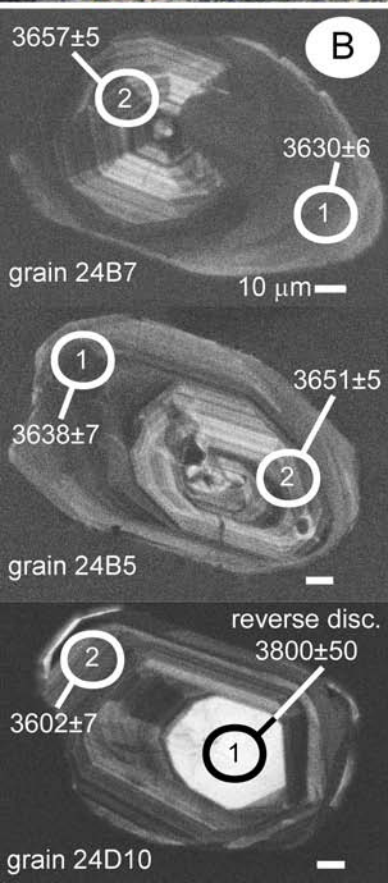
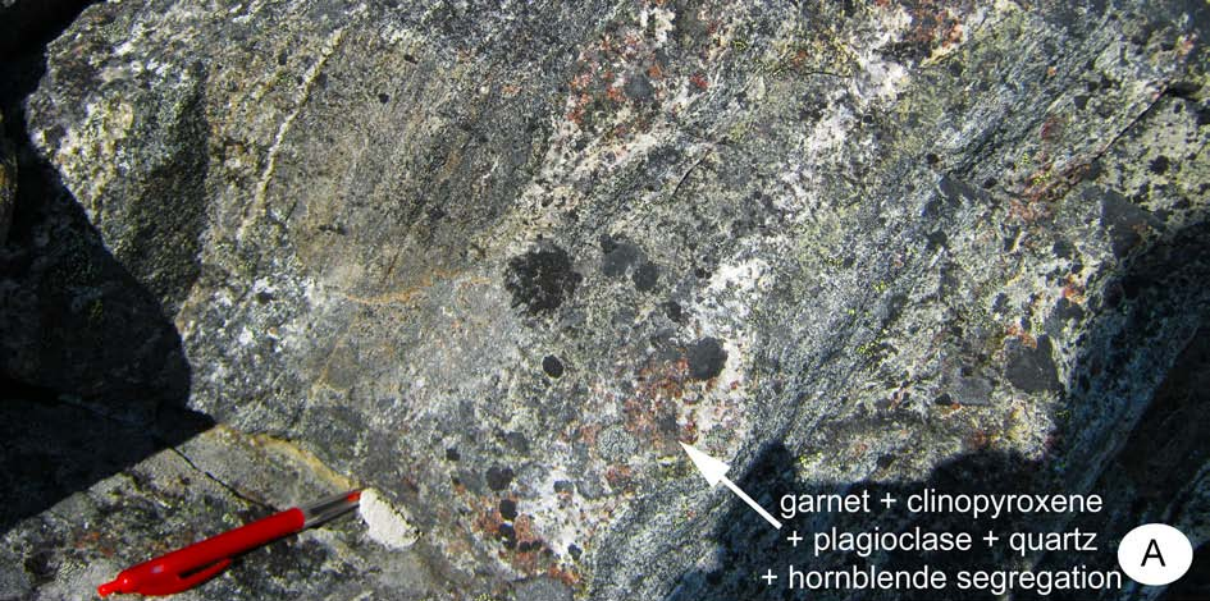
mixed; in lower crust (3.89-3.66 Ga) - strongly deformed and intercalated

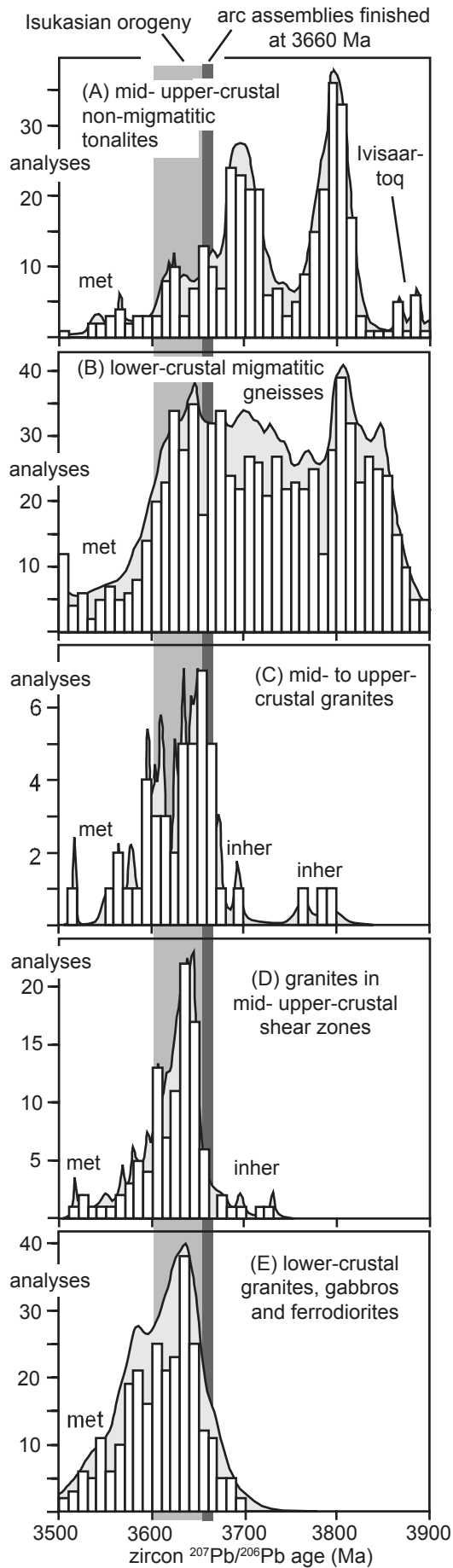


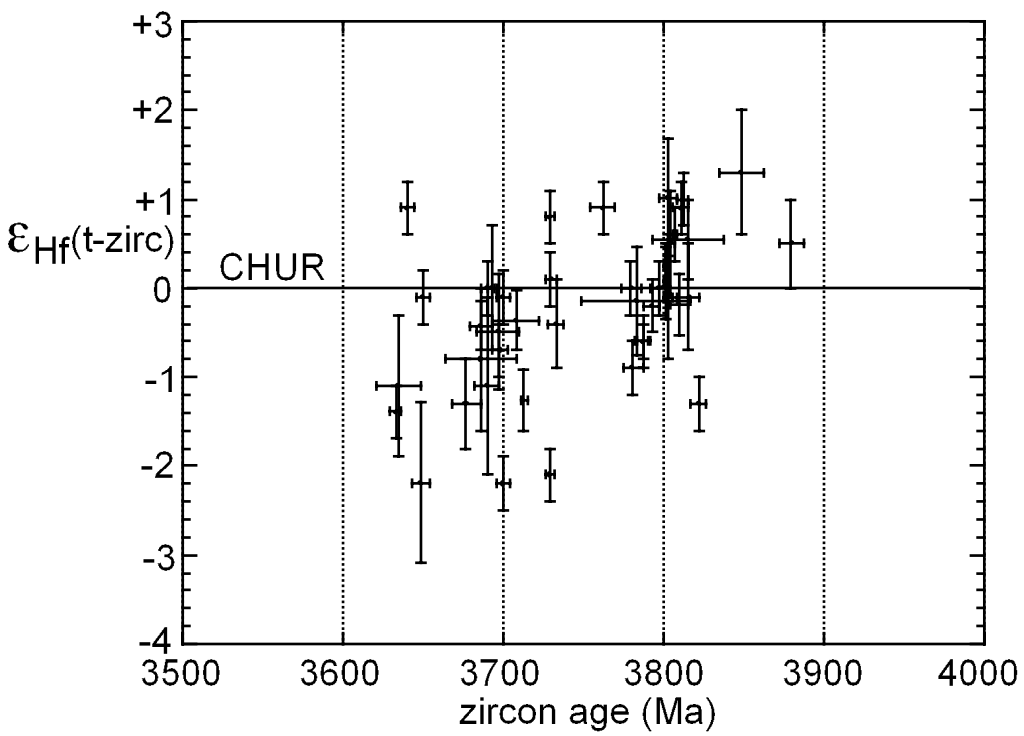












Spot	site	ppm U	ppm Th	Th/U	% 206Pb _c	238U /206Pb* ±%	207Pb* /206Pb* ±%	207Pb /206Pb age	% Dis- cor- dant
24A-1.1	e,osc,eq	56	0.50	0.009	0.19	1.268 1.3	0.3372 0.49	3650 ±7	-4
24A-2.1	e,osc,eq	116	0.65	0.006	0.10	1.327 1.0	0.3390 0.33	3658 ±5	+1
24A-3.1	<i>e,osc+rex,eq</i>	<i>84</i>	<i>1.26</i>	<i>0.015</i>	<i>0.10</i>	<i>1.286 1.1</i>	<i>0.3374 0.39</i>	<i>3651 ±6</i>	<i>-2</i>
24A-4.1	e,h/rex,p	152	1.95	0.013	0.08	1.308 0.9	0.3351 0.30	3641 ±5	-1
24A-4.2	<i>m,osc+rex,p</i>	<i>61</i>	<i>1.83</i>	<i>0.030</i>	<i>0.13</i>	<i>1.341 1.3</i>	<i>0.3369 0.47</i>	<i>3649 ±7</i>	<i>+2</i>
24A-5.1	e,osc,p	64	1.19	0.019	0.12	1.319 1.3	0.3407 0.46	3666 ±7	+1
24A-5.2	m,rex,p	7	0.70	0.099	1.56	1.515 3.7	0.3310 1.83	3622 ±28	+12
24A-6.1	e,rex,eq	35	1.23	0.035	0.34	1.317 1.8	0.3345 0.73	3638 ±11	-0
24A-7.1	e,osc,p	17	0.30	0.018	1.38	1.332 2.5	0.3374 1.25	3651 ±19	+1
24A-8.1	<i>e,osc+rex,eq</i>	<i>64</i>	<i>0.19</i>	<i>0.003</i>	<i>0.02</i>	<i>1.279 1.3</i>	<i>0.3372 0.46</i>	<i>3650 ±7</i>	<i>-3</i>
24A-9.1	e,rex,p	46	0.51	0.011	0.20	1.313 1.5	0.3332 1.00	3632 ±15	-1
24A-10.1	e,h/rex,p	33	0.55	0.017	0.36	1.355 1.8	0.3307 0.73	3620 ±11	+2
24A-11.1	e,h/rex,p	36	0.15	0.004	0.15	1.283 1.6	0.3339 0.60	3635 ±9	-3
24A-11.2	m,osc,p	13	0.13	0.010	0.35	1.345 2.5	0.3409 1.00	3667 ±15	+3
24A-12.1	e,h/rex,p	60	0.56	0.009	0.08	1.318 1.2	0.3317 0.45	3625 ±7	-1
24A-12.2	m,rex/osc,p	4	0.19	0.044	1.39	1.450 4.7	0.3413 2.27	3668 ±35	+10
24A-13.1	m,osc,p	129	0.51	0.004	0.02	1.345 0.9	0.3407 0.31	3666 ±5	+3
24A-14.1	m,osc,p	85	0.16	0.002	0.12	1.352 1.1	0.3410 0.40	3667 ±6	+3

24A-15.1	e,sz,p	94	1.64	0.017	0.32	1.286	1.4	0.3245	0.54	3591	±8	-4
24A-15.2	e,osc,p	21	0.27	0.013	0.31	1.301	2.0	0.3412	0.84	3668	±13	-0
24B-1.1	<i>e,h+osc,p</i>	50	0.18	0.004	0.16	1.326	1.5	0.3338	0.55	3634	±8	+0
24B-2.1	e,h,p	269	5.18	0.019	0.09	1.384	0.8	0.3244	0.23	3591	±4	+3
24B-2.2	m,rex/h,p	10	0.23	0.022	1.37	1.731	3.4	0.3470	1.93	3694	±29	+25
24B-3.1	e,osc,eq	109	0.16	0.001	0.09	1.304	1.0	0.3377	0.36	3652	±5	-1
24B-4.1	e,sz,p	83	1.02	0.012	0.06	1.351	1.2	0.3303	0.43	3618	±7	+2
24B-5.1	e,sz,p	76	0.60	0.008	0.02	1.329	1.2	0.3345	0.45	3638	±7	+1
24B-5.2	e,osc,p	153	0.21	0.019	0.03	1.314	0.9	0.3373	0.32	3651	±5	+0
24B-6.1	e,sz,p	95	1.80	0.019	0.06	1.288	1.1	0.3326	0.40	3629	±6	-3
24B-7.1	e,sz/rex,p	94	2.67	0.028	0.10	1.345	1.1	0.3328	0.39	3630	±6	+2
24B-7.2	m,osc,p	109	0.67	0.006	0.04	1.293	1.0	0.3388	0.35	3657	±5	-1
24B-8.1	e,sz,p	281	1.42	0.005	0.05	1.442	1.0	0.2532	0.22	3205	±4	-8
24B-8.2	m,osc,p	78	1.01	0.013	0.72	1.269	1.2	0.3381	0.50	3654	±8	-3
24B-10.1	e,osc,eq,fr	67	1.30	0.019	0.13	1.287	1.2	0.3381	0.45	3654	±7	-2
24B-11.1	e,sz,p	71	0.29	0.004	0.05	1.359	1.2	0.3225	0.43	3582	±7	+1
24B-11.2	m,osc,p	17	0.73	0.042	0.18	1.300	2.3	0.3455	0.86	3687	±13	+0
24B-12.1	<i>e,rex+osc,p</i>	66	0.48	0.007	0.15	1.332	1.2	0.3366	0.45	3648	±7	+1
24B-12.2	m,osc,p	197	0.30	0.002	0.05	1.348	0.8	0.3381	0.25	3654	±4	+3
24B-12.3	e,osc,p	110	0.56	0.005	0.15	1.246	1.0	0.3361	0.37	3645	±6	-6
24B-13.1	m,h,eq,fr	9	0.26	0.029	1.47	1.357	2.9	0.3246	1.39	3592	±21	+1

24B-13.2	e,h,eq,fr	82	1.92	0.023	0.07	1.287	1.1	0.3336	0.40	3634	±6	-3
24B-14.1	e,h/rex,p	62	2.17	0.035	0.19	1.271	1.3	0.3321	0.49	3627	±7	-4
24B-14.2	m,osc,p	88	1.00	0.011	0.05	1.334	1.1	0.3384	0.38	3656	±6	+2
<i>24B-15.1</i>	<i>e,h/rex2,eq</i>	<i>216</i>	<i>2.51</i>	<i>0.012</i>	<i>0.08</i>	<i>1.452</i>	<i>0.8</i>	<i>0.3326</i>	<i>0.43</i>	<i>3629</i>	<i>±7</i>	<i>+9</i>
24B-15.2	m,osc,eq	50	1.26	0.026	0.13	1.284	1.5	0.3392	0.59	3659	±9	-2
24B-9.1	m,osc,eq	85	0.33	0.004	0.08	1.300	1.1	0.3377	0.38	3652	±6	-1
24C-1.1	e,sz,p,fr	76	0.82	0.011	0.25	1.345	1.2	0.3260	0.47	3598	±7	+1
24C-1.2	m,osc,p,fr	105	0.23	0.002	0.08	1.286	1.0	0.3362	0.35	3646	±5	-2
24C-2.1	e,sz,p,fr	558	6.06	0.011	0.22	3.329	0.7	0.2947	0.29	3442	±4	+57
24C-2.2	e,sz,p,fr	166	0.56	0.003	0.05	1.483	0.9	0.3353	0.31	3642	±5	+11
24C-2.3	m,osc,p,fr	84	0.46	0.005	0.07	1.324	1.1	0.3376	0.41	3652	±6	+1
24C-3.1	e,h/rex,p	250	0.81	0.003	0.03	1.328	0.8	0.3340	0.41	3636	±6	+1
24C-3.2	m,osc,p	73	0.86	0.012	0.09	1.377	1.2	0.3389	0.43	3658	±7	+5
24C-3.3	e,h/rex,p	213	1.64	0.008	0.11	1.315	0.8	0.3352	0.25	3641	±4	-0
24C-4.1	e,h/rex,p	227	2.96	0.013	0.09	1.538	0.8	0.3275	0.26	3606	±4	+13
24C-4.2	m,h/rex,p	1126	14.30	0.013	0.02	1.378	0.6	0.3303	0.11	3618	±2	+4
24C-5.1	e,osc,p,fr	98	0.31	0.003	0.11	1.310	1.0	0.3372	0.36	3650	±5	-0
24C-5.2	m,osc,p,fr	131	3.57	0.027	0.04	1.296	0.9	0.3406	0.30	3666	±5	-1
<i>24C-6.1</i>	<i>m,osc+rex,eq</i>	<i>90</i>	<i>0.54</i>	<i>0.006</i>	<i>0.08</i>	<i>1.333</i>	<i>1.0</i>	<i>0.3366</i>	<i>0.37</i>	<i>3648</i>	<i>±6</i>	<i>+1</i>
24C-7.1	e,h/rex,p	202	1.78	0.009	0.02	1.304	0.8	0.3337	0.24	3634	±4	-1
24C-7.2	m,osc,p	50	0.28	0.006	0.07	1.292	1.4	0.3396	0.50	3661	±8	-1

24C-8.1	m,osc,p	27	0.74	0.027	0.30	1.295	1.7	0.3378	0.69	3653	±11	-1
24C-8.2	e,h/rex,p	88	2.01	0.023	0.06	1.272	1.1	0.3326	0.39	3629	±6	-4
24C-9.1	e,rex,p	224	0.25	0.001	0.04	1.304	0.8	0.3363	0.23	3646	±4	-1
24C-9.2	m,osc,p	54	0.26	0.005	0.18	1.325	1.3	0.3462	0.48	3690	±7	+2
24C-10.1	e,h/rex,p,fr	469	1.48	0.003	0.04	2.896	1.0	0.2830	0.61	3380	±9	+50
24C-10.2	m,osc,p,fr	96	0.28	0.003	0.09	1.292	1.0	0.3383	0.36	3655	±5	-1
24C-10.3	m,rex,p,fr	234	1.44	0.006	0.04	1.320	0.8	0.3331	0.23	3631	±4	-0
24C-10.4	m,rex,p,fr	5	0.07	0.014	0.68	1.400	3.8	0.3314	2.45	3624	±38	+5
24C-11.1	e,h/rex,p	174	1.25	0.007	0.09	1.342	0.8	0.3356	0.27	3643	±4	+2
24C-11.2	e,h/rex,p	720	2.00	0.003	0.03	1.376	0.6	0.3310	0.13	3622	±2	+4
24C-11.3	m,h/rex,p	4008	1.39	0.000	0.60	9.173	0.8	0.1421	2.13	2253	±37	+74
24D-2.2	e,h/rex,eq	122	0.42	0.003	0.17	1.574	1.0	0.3276	0.36	3606	±6	+15
24D-1.1	m/c,osc,p	20	0.08	0.004	0.66	1.317	2.2	0.3453	0.89	3686	±14	+2
24D-1.2	e,h/rex,p	48	0.96	0.020	0.26	1.344	1.4	0.3258	0.57	3597	±9	+0
24D-2.1	e,h/rex,eq	1	0.02	0.044	9.23	1.557	17.6	0.4490	8.40	4082	±125	+27
24D-3.1	m,h/rex,p	2	0.04	0.018	3.67	1.367	6.3	0.3031	5.36	3486	±83	-2
24D-4.1	m,osc,p	35	0.19	0.006	0.16	1.314	1.6	0.3374	0.62	3651	±9	+0
24D-4.2	<i>e,osc+rex,p</i>	<i>1515</i>	<i>1.42</i>	<i>0.001</i>	<i>0.14</i>	<i>1.963</i>	<i>1.3</i>	<i>0.2038</i>	<i>0.45</i>	<i>2857</i>	<i>±7</i>	<i>+9</i>
24D-5.1	e,osc,p	87	0.49	0.006	0.14	1.312	1.2	0.3262	0.43	3599	±7	-2
24D-5.2	m,rex/h,p	9	0.22	0.024	0.45	1.297	3.0	0.3345	1.22	3638	±19	-2
24D-6.1	m,osc,p	13	0.32	0.025	0.42	1.308	2.5	0.3382	1.00	3655	±15	-0

24D-6.2	e,h/rex,p	77	0.38	0.005	0.05	1.303	1.1	0.3331	0.41	3631	±6	-1
24D-7.1	m,rex,eq	6	0.05	0.009	2.70	1.380	4.0	0.3187	2.31	3564	±36	+2
24D-7.2	e,rex,eq	128	0.92	0.007	0.12	1.271	0.9	0.3332	0.32	3632	±5	-4
24D-8.1	m,osc,eq	8	0.08	0.010	1.15	1.401	3.2	0.3407	2.51	3666	±38	+7
24D-8.2	e,rex,eq	293	0.68	0.002	0.22	1.548	0.7	0.2908	0.26	3422	±4	+8
24D-9.1	m,rex+osc,p	8	0.03	0.003	2.07	1.353	3.3	0.3496	1.62	3705	±25	+5
24D-9.2	e,h/rex,p	64	1.35	0.021	0.18	1.281	1.2	0.3321	0.47	3627	±7	-3
24D-10.1	m,rex,p	3	0.09	0.036	3.56	1.366	6.0	0.3720	3.33	3800	±50	+9
24D-10.2	e,rex+osc,p	82	0.18	0.002	0.19	1.301	1.2	0.3268	0.48	3602	±7	-3
24D-11.1	m,osc,eq	19	0.03	0.001	0.37	1.413	2.3	0.3381	0.98	3654	±15	+7
24D-11.2	e,osc+rex,eq	89	0.59	0.007	0.03	1.301	1.1	0.3376	0.38	3652	±6	-1
24D-12.1	m,osc+rex,p	2	0.08	0.038	1.08	1.287	6.1	0.3463	2.59	3691	±39	-1
24D-12.2	e,h/rex,p	98	1.04	0.011	0.02	1.285	1.0	0.3372	0.36	3650	±6	-2
24D-13.1	m,osc,p	35	0.19	0.005	0.20	1.281	1.6	0.3386	0.62	3657	±9	-2
24D-13.2	e,rex/h,p	85	1.91	0.023	0.08	1.400	1.1	0.3141	0.41	3541	±6	+2
24D-14.1	e,rex,p,fr	68	0.36	0.005	0.30	1.328	1.3	0.3314	0.84	3624	±13	+0
24D-15.1	m,rex,p	6	0.02	0.004	0.49	1.289	3.7	0.3643	1.44	3768	±22	+2
24D-15.2	e,h/rex,p	76	0.94	0.012	0.07	1.273	1.2	0.3341	0.41	3636	±6	-4
24D-16.1	m,rex/h,p	3	0.02	0.007	1.54	1.530	5.0	0.3553	4.66	3730	±71	+17
24D-16.2	e,rex+osc,p	65	0.34	0.005	0.06	1.322	1.2	0.3373	0.43	3651	±7	+1
24D-17.1	e,rex+osc,p	39	0.97	0.025	0.39	1.315	1.5	0.3376	0.95	3652	±15	+0

24D-18.1	m,osc,p	97	1.37	0.014	0.04	1.296	1.0	0.3376	0.34	3652	±5	-1
24D-18.2	e,rex/h,p	73	0.51	0.007	0.07	1.265	1.2	0.3335	0.43	3633	±7	-4
<i>24D-19.2</i>	<i>e,rex+osc,p</i>	<i>43</i>	<i>0.71</i>	<i>0.016</i>	<i>0.09</i>	<i>1.294</i>	<i>1.4</i>	<i>0.3364</i>	<i>0.52</i>	<i>3646</i>	<i>±8</i>	<i>-2</i>
24D-20.1	m,rex/h,p	12	0.03	0.003	0.38	1.456	2.7	0.3449	2.54	3685	±39	+11
24D-19.1	m,rex/h,p	26	2.66	0.103	28.00	0.951	13.9	0.2035	67	2855	±1092	-89
24D-20.2	m,rex/h,p	330	5.30	0.016	0.41	1.582	0.8	0.3224	0.32	3581	±5	+15
24D-21.1	e,sz,p	29	0.47	0.016	0.41	1.284	1.8	0.3332	0.79	3632	±12	-3
24D-22.1	e,rex,p	100	0.55	0.006	0.07	1.291	1.0	0.3369	0.36	3649	±5	-2
24D-23.1	m,osc,p	17	0.06	0.003	0.34	1.331	2.2	0.3422	0.85	3673	±13	+2
<i>24D-23.2</i>	<i>e,osc+rex,p</i>	<i>106</i>	<i>0.78</i>	<i>0.007</i>	<i>0.26</i>	<i>1.286</i>	<i>1.1</i>	<i>0.3364</i>	<i>0.38</i>	<i>3646</i>	<i>±6</i>	<i>-2</i>

zircon morphology and analysis site: p=prism; e=equant grain; fr=grain fragment; e=grain end; m=mid-grain

CL petrography: osc=oscillatory zoned; h=homogeneous, sz=sector zoned; rex=recrystallized

analyses in italics are ones with composite domains, and not used in age determinations

%206Pbc = percentage of 206Pb determined to be of non radiogenic origin, based on measured 204Pb/206Pb ratio and

Cumming and Richards model Pb compositions